

POLITECNICO DI TORINO

SCUOLA INTERPOLITECNICA DI DOTTORATO

Nanotecnologie e Materiali Innovativi Nanostrutturati

*Microfluidic for human health: a versatile tool  
for new progress in cancer diagnosis and  
contaminants detection*



*Giorgia Celetti*

Tutor  
prof. \_\_\_\_\_

Co-ordinator of the Research Doctorate Course  
prof. Barbara Bonelli

March 2013/January 2016



*Dedicate to who believe in himself*

---

# *Table of contents*

## *Abstract*

### **1. *General introduction and thesis outline***

#### *1.1 Microdroplets in Microfluidics: an evolving platform for cell biology and sensing*

##### *1.1.1 Key characteristics of microdroplets in microfluidics*

#### *1.2 Droplet microfluidics*

#### *1.3 Droplet microfluidics applications*

##### *1.3.1 Droplet microfluidics: a tool for single-cells analysis*

###### *1.3.1.1 Circulating tumor cells detection*

##### *1.3.2 Droplet microfluidic: a platform for functional microparticles production for detection applications.*

###### *1.3.2.1 Poly(ethylene glycol) (PEG) microparticles*

###### *1.3.2.2 Microfluidics for food analysis: aflatoxin M1*

#### *1.4 Outline of Dissertation*

### **2. *A microfluidic approach for single-cell metabolism determination, a tool for circulating tumor cells detection***

#### *2.1 Introduction*

#### *2.2 Results and discussion*

##### *2.2.1. Characterization using cell lines*

##### *2.2.2. Outperforming other methods*

##### *2.2.3. Optimization: A549 mixed to WBC for clinical samples simulation*

##### *2.2.4. Capture of cancer cells from blood sample of patients*

#### *2.3 Conclusions*

#### *Acknowledgments*

#### *2.4 Experimental Section*

#### *References*

### ***3. Microfluidic synthesis of Peptide-functionalized microgels for in serum selective protein detection***

*3.1 Introduction*

*3.2 Results and discussion*

*3.2.1. Microfluidic design*

*3.2.2. PEGDA peptide-microgels synthesis and characterization*

*3.2.3. Protein-binding analysis in PBS and human serum*

*3.3 Conclusions*

*Acknowledgments*

*3.4 Experimental Section*

*References*

### ***4. Label-free method for aflatoxin detection: microfluidic microgels functionalized with two novel peptides***

*4.1 Introduction*

*4.2 Results and discussion*

*4.2.1. Peptides sequences characterization*

*4.2.2. Biosensing development*

*4.3 Conclusions*

*Acknowledgments*

*4.4 Experimental Section*

*References*

### ***5. Conclusions and perspectives***

*5.1 Conclusion and outlook*

*References*

***Acknowledgments***

---

## *Abstract*

In the last ten years, interest in manipulating droplets in microchannels has emerged from two important motivations. The first arise from the desire to produce well controlled droplets for material science applications, for example in the pharmaceutical or food industries. In this context, microfluidics allows for producing such droplets in a controlled and reproducible manner, also allowing complex combinations to be designed and explored. A second motivation originates with the advent of the -omics era, which has a much need for being able to carry out experiments at the smallest possible scale (if possible single cells or molecules), on a massively parallel platform and with high throughput. In this case, droplets are viewed as micro-reactor in which samples are confined, and which offer a way to manipulate small volumes.

Droplet microfluidics is the most powerful microfluidic technology used to produce and manipulate monodisperse droplets. This technique addresses the need for lower costs, shorter times, and higher sensitivities to compartmentalize reactions into picolitre volume, instead of the microlitre volumes commonly used with standard methods.

Droplets can provide a well-defined environment into which individual cells can be compartmentalized in a controlled way. This coupled with the advantages of droplet microfluidics has allowed the development of several methods for single-cells analysis. In this work a microfluidics label-free approach for circulating tumor cells (CTCs) detection is presented. In the last decades, CTCs have received enormous attention as a new biomarkers for cancer study, for this reason their capture and retain represents a major challenge in cancer research. Many issues regarding the detection and characterization of CTCs are owing to their extremely rarity (one CTCs for  $5 \times 10^9$  erythrocytes/mL and for  $7 \times 10^6$  leucocytes /mL) and their heterogeneous nature (there is no unique biologic marker for CTCs identification). Although much promising progress has been made in CTCs detection, the robustness in distinguishing between healthy cells and CTCs, and the isolation of live CTCs need to be improved further. The method developed in this work exploits the so-called Warburg effect (WE): even in the presence of oxygen cancer cells limit largely their metabolism to glycolysis leading to increased production of lactate. Using droplet microfluidics, cancer cells are compartmentalized into a picolitre droplets and lactate secreted by cells are retained in the droplet. The secretion of lactate leads to a rapid increase in the concentration of acid in cell-containing droplets. CTCs are thus detected by monitoring the pH of the droplet using a pH-sensitive dye, without the need for surface-antigen labeling. A suspension of tumor cells

---

(A549) mixed with white blood cells were emulsified in picoliter droplets, and it was observed a clear fraction of droplets with a reduced pH, leading to a distinct population of droplets containing a cancer cell from empty or WBC containing drops. With this method a very few number (up to 10) of tumor cells in a background of 200,000 white blood cells are detected, with average detection rates in the range of 60%. To demonstrate that this is a general method for detection of cancer cells, several cancer cell lines were tested, including ovarian TOV21G, breast MDA-MB 453, glioblastoma U231, colorectal HT-29, breast MCF-7 and MDA-MB-231 and all showed acidification of droplets. With the method established, samples based on blood cancer patients with confirmed metastatic disease were tested. The results show clearly that numerous positive droplets are detected in the sample of metastatic patients. Moreover, this method is capable of retrieving live cells, opening up routes for further large scale investigation of the nature of CTCs.

Another interesting area where droplet-based microfluidics is playing an increasingly important role is the synthesis of functional polymeric microparticles or microgels. They have been suggested as diagnostic tools for the rapid multiplexed screening of biomolecules, because of their advantages in detection and quantification.

In the second part of this thesis, the synthesis of polymeric microparticles, functionalized with peptides, through droplet microfluidics is presented. Peptide was efficiently encapsulated into the polymeric microparticles in order to create a functional microparticles for selective protein detection in complex fluids. Protein binding occurred with higher affinity ( $K_D$  0.1-0.4  $\mu\text{M}$ ) than the conventional detection methods ( $K_D$  70  $\mu\text{M}$ ). Current work demonstrate easy and fast realization of functionalized monodisperse microgels using droplet microfluidic and how the inclusion of small molecules within polymeric network improve both the affinity and the specificity of protein capture. This work provides advances in gel particle functionalization and opens new possibilities for direct molecules detection in complex fluids. A possible application of this method was for label-free aflatoxin  $M_1$  (AFM<sub>1</sub>) detection. AFM<sub>1</sub> is the most toxic, carcinogenic, teratogenic and mutagenic class of aflatoxins (AFs) and can be present due to <fungal contamination> in a wide range of food and feed commodities, such as milk and dairy products, representing an important issue especially for developing countries. Currently, the detection methods used to quantify AFM<sub>1</sub> require complex and laborious sample pretreatments, expensive instruments and skilled operators, thus limiting their application. Driven by the need of overcoming some of these limits, poly(ethylene glycol) dyacrilate (PEGDA) functional microparticles were produced using microfluidics. Two novel

peptides were synthesized for specific aflatoxin detection and encapsulated in PEGDA microparticles for AFM<sub>1</sub> detection. AFM<sub>1</sub>-binding peptides occurred with high affinity ( $K_D$  3.66-6.57 pM, respectively for the two sequences) and detection was achieved measuring AFM<sub>1</sub> innate fluorescence. The detection limit of this technique for AFM<sub>1</sub> was estimated to be 1.64 ng/Kg, with a dynamic detection range between 3.28 ng/Kg and 70 ng/Kg, which meets present legislative limits of 50 ng/Kg for AFM<sub>1</sub> in milk. Therefore, the developed systems provides a promising approach for rapid screening of food contaminates because it resulted to be simple, sensitive, specific, and with not need multiple separation steps, overcoming the limits of the traditional AFM<sub>1</sub> detection methods, which are expensive and time consuming. The use of microfluidics has allowed development of robust, label-free, sensitive and high-throughput platforms which may be used in the near future to improve the quality of life.

---

## CHAPTER 1

### *General introduction and thesis outline*

*Academics like complexity and emergency. The real world puts up with it reluctantly, but really wants simplicity....*

*...whatever simplicity is.*

*(G. Whitesides).*

*You know you've achieved perfection in design, not when you have nothing more to add, but when you have nothing more to take away.*

*(de Saint-Exupery)*

---

## 1.1 *Microdroplets in Microfluidics: an evolving platform for cell biology and sensing*

In 1954 Joshua Lederberg published a “simple method for isolating individual microbes”<sup>1</sup>, demonstrating the compartmentalization of single cells into nanoliter droplets. However, although the basic ideas of compartmentalization of cells and the study of enzymatic reactions in microdroplets were demonstrated, it has taken almost 50 years for Lederberg’s vision to become reality. With the advent of the -omics era there is an apparent need arisen for being able to carry out experiments at the smallest possible scale (single cells or molecules), on a massively parallel platform and with high throughput<sup>2</sup>. Recent advances in microfluidics have enabled the development of powerful tools for manipulation small amount ( $10^{-6}$  to  $10^{-12}$  litres) of volume in channels at length scales of tens to hundreds of micrometers<sup>3</sup>. Microfluidics coupled with the technologies developed by the micro-electromechanical systems (MEMS) field have provided the possibility to build up extremely reproducible and well defined fluidic chips, commonly referred as micro-total analysis systems (uTASs)<sup>4,5</sup> or Lab-on-a-chip (LOC). This combination has resulted in a rapidly growing interest by researches to use microfluidic microdroplets for cell biology and biosensing applications<sup>2,6-8</sup>. The key features of microparticles in microfluidics are that they are monodisperse in size and therefore potentially suitable for carrying out quantitative studies, provide a compartment in which species can be isolated, provide the possibility to work with extremely small volumes and single cells or molecules, and offer to perform very large numbers of experiments<sup>2</sup> (figure 1.1). These specific features have enabled the use of microdroplets as tools for discoveries in cell biology and bio-detection.

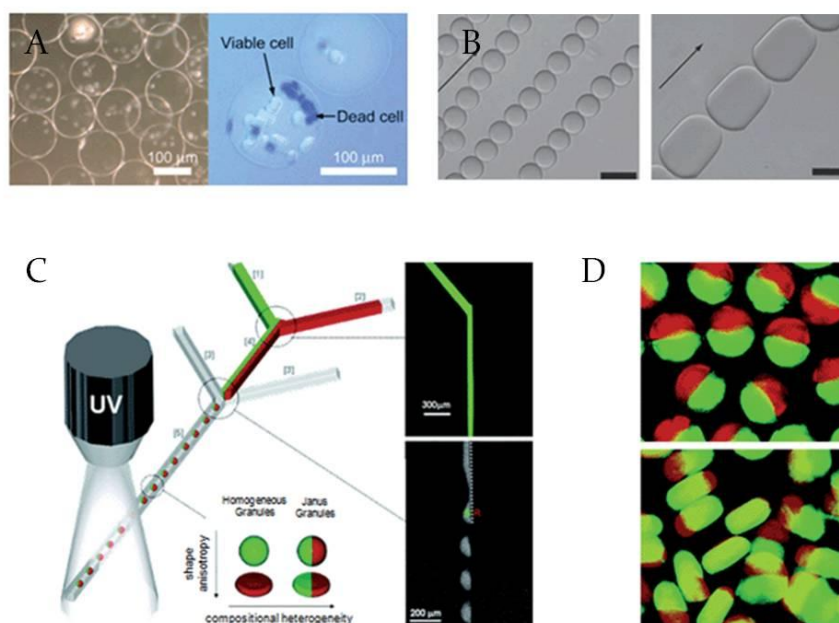


**Figure 1.1:** Microdroplets in microfluidics: A) microdroplets for single-cells analysis; B); C) droplet microfluidics for functional microparticles production; D) Dual fluorescence colloid-filled hydrogel granules (“Janus” particles). Reproduced with permission from ref [ ]

### 1.1.1 Key characteristics of microdroplets in microfluidics

#### **Compartmentalization, monodispersity, small, fast reactions**

The compartmentalization of reactions in microdroplet can be applied to a very wide range of experiments, chemical or biological. For example, in experiments where droplets contain single cell or living organisms, the environment of the cell can be controlled and its changes can be measured and studied. Microdroplets prepared through microfluidic platforms are highly monodisperse, with polydispersities in the range of 1 % (in diameter)<sup>9,10</sup>. Thus every experiment took place in the same volume, controlling the concentration of reagents and reaction products. Furthermore, the analysis of reactions in bulk emulsions by screening individual droplets takes a considerable amount of time and therefore every droplet is analyzed at a different reaction time. With microfluidics, the screening is not much faster, but the rank order of droplets can be maintained and so every droplet has the same time lag between formation and screening. Additionally, droplets can be analyzed directly on-chip using integrated techniques, such as fluorescence detection, so they can be analyzed at controlled times<sup>11-13</sup>. The advantage of microfluidic technologies is crucial: as monodisperse droplets are formed on-chip and reactions are initiated at the point of drop formation or by droplet fusion, every droplet is identical in terms of concentrations and time-analysis. This has an important advantage in single-cell or single-molecule

studies, where stochastic variations require the detailed analysis and combination of data from large numbers of experiments<sup>14</sup>.

Typical droplet volumes are in the nanoliter (nL) to picoliter (pL) range. As a result, reagent consumption is extremely small, allowing for the screening and analysis of precious compounds. Controlling the volume of droplets, the ability to tune the concentration of macromolecules in droplets also provides an ideal platform for exploring optimum conditions for protein crystallization<sup>12,15</sup>. Moreover, the confinement of a single cells in droplets allows released molecules to accumulate in a small compartment, their concentration hence rapidly increases into droplet, and the time required to detect the released molecules is reduced<sup>16</sup>.

## 1.2 Droplet microfluidics

Droplet-based microfluidics involves the generation and manipulation of monodisperse droplets, which can serve as compartments for single cell analysis or can be polymerized into polymeric microparticles for diagnostics and biosensing<sup>17</sup>. Unlike continuous flow systems, droplets enable isolated reactions to be performed in parallel without cross-contamination or sample dilution. Microfluidic droplet-based systems represent a high-throughput platform for biological and chemical research<sup>18,19</sup>. The formation of droplets can be done with passive mechanisms, such as with co-flowing streams, cross-flowing streams in a T-shaped junction, and elongation flow in a flow focusing (FF) geometry<sup>20</sup> (figure 1.2) or with active electrohydrodynamic (EHD) mechanisms, such as dielectrophoresis (DEP)<sup>21</sup> and electrowetting on dielectric (EWOD)<sup>22</sup>.

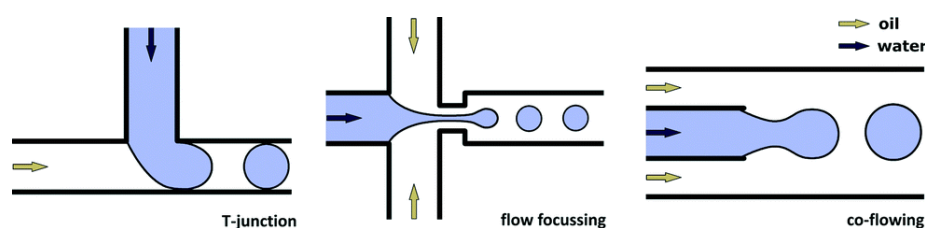


**Figure 1.2:** Standard geometries used for controlled droplet formation in microfluidic devices – T-junction, Flow-focusing Device (FFD) and Co-flow. Reproduced with permission from

Generally, two immiscible liquids such as a hydrophilic solution and hydrophobic oil are combined at a rate in which the shear force at the fluid interface is sufficiently large to cause the continuous phase to break the aqueous phase into discrete droplets<sup>23,24</sup>. The dimensionless Capillary number (Ca) plays a key role in droplet break-off. Droplet

formation is driven by the competition between the viscous stress and the surface tension of the two immiscible fluids, and occurs at a critical Ca:  $Ca = \frac{\eta U_0}{\gamma}$ , where  $\eta$  [Pa-s] and  $U_0$  [m/s] are the viscosity and velocity of the continuous phase, respectively, and  $\gamma$  [N/m] is the interfacial tension between the immiscible phases<sup>25,26</sup>. Above a certain critical capillary number, droplet break off occurs. A low value of Ca indicates that the stresses due to interfacial tension are strong compared to viscous stress. Drops flowing under such a condition nearly minimize their surface area by producing spherical ends. In the opposite situation of high Ca, viscous effects dominate and one can observe large deformations of the drops and asymmetric shapes<sup>26</sup>. It is important to note that the critical capillary number is system dependent as different values have been reported by various groups using different geometries. To realize this number, it is important to consider the relative viscosity between the two phases. Selection of a more viscous hydrophobic phase will facilitate formation of droplets<sup>20</sup>. For example, for water-in-oil (W/O) emulsion, hydrophobic phase commonly consists of oils, which tends to be naturally more viscous than water. The immiscibility of the two-phases ensures the isolation and compartmentalization of each phase.

Passive droplet generation techniques are ideal for experimental conditions where a large number of droplets are desired, namely for high-throughput or parallel analysis applications, such as large-scale PCR<sup>27</sup> or culturing techniques<sup>28</sup>. Furthermore, the composition of the neighboring droplets can be controlled by adjusting the relative concentration of the upstream aqueous solution. This is especially useful for chemical analysis applications, such as enzymatic assays<sup>29</sup>, drug discovery assays<sup>30</sup> and protein crystallization techniques<sup>12</sup>.

### ***1.3 Droplet microfluidics applications***

The high control and integrative ability available for operating and manipulating droplets make droplet microfluidic technology ideal for biomedical and biotechnology applications. In particular, the areas where droplet-based microfluidic platforms are playing an increasingly important role and of interest for this thesis are the analysis at single cell level and the synthesis of functional hydrogel microparticles for biosensing and detection<sup>31</sup>.

### *1.3.1 Droplet microfluidics: a tool for single-cells analysis*

Droplet microfluidics allows the isolation of single cells in a well-defined (potential sterile) environment and the manipulations at a throughput of thousands of droplets per second<sup>32</sup>. A strong advantage of analyzing single cells in droplets is the ability of rapid detection of cell-secreted molecules due to the low volume surrounding each encapsulated cell, thereby overcoming one of the major limitations of traditional flow cytometry (FC) and fluorescence-activated cell sorting (FACS)<sup>33</sup>. In addition, in microfluidic systems, droplets can be merged with other droplets<sup>34</sup>, split into two<sup>35</sup> or dielectrophoresis (DEP)-sorted<sup>36</sup> for further analysis.

The growing of emerging technologies have enabled to integrate electrodes into microdevices providing electrical control over droplet motion and manipulation<sup>20</sup>. For examples the integration of DEP-based sorting in droplet microfluidics has allowed to retrieve a specific subset of droplets from the rest of the droplet stream. The retrieval of a small population of cells for further analysis is a crucial step in cases of circulating tumor cells, hybridoma production or drug screening. Recently, DEP combined with laser-induced fluorescence (LIF) technique has allowed to separate target droplets from the rest of the droplet stream with electric fields according to their fluorescent content, thereby isolating the droplets of interest<sup>36-38</sup>. LIF is a spectroscopy method that offer very sensitive and ultra fast detection in many applications such as cell-based assays, PCR detection and binding assay<sup>39</sup>.

Griffiths, Weitz and coworkers showed an example of integrated on-chip fluorescent-activated droplet sorting system, based on DEP-sorting, for high-throughput analysis of single cells (figure 1.3). They described a binding assay to detect antibodies secreted from single mouse hybridoma cells. Secreted antibodies were detected by co-compartmentalizing single mouse hybridoma cells, a fluorescent probe and single beads coated with anti-mouse IgG antibodies in 50 pL droplets. When the binding occurs a clearly distinguishable signal of fluorescence inside droplet is generated and recorded by laser. If the intensity of the fluorescence is above a preselected threshold such droplet is actively sorted via DEP<sup>40</sup>.

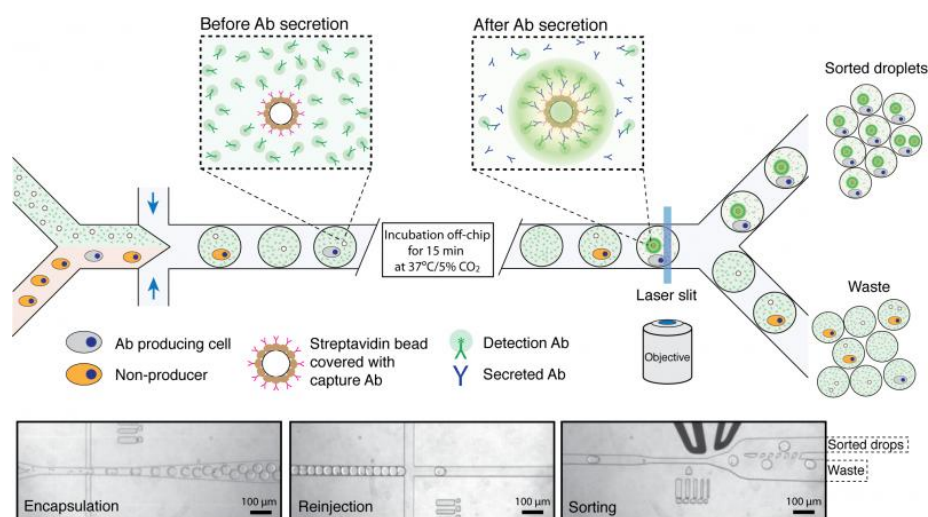


**Figure 1.3:** Integrated on-chip fluorescent-activated droplet sorting system, based on DEP-sorting, for high-throughput analysis of single cells. Three steps are describe:1) cells encapsulation; 2) droplets containing cells reinjection in a second device; 3) droplets containing green fluorescent beads are sorted using a fluorescence activated droplet sorter. Reproduced with permission from Ref [40]

Single cell is the fundamental component of life, therefore, single-cell analysis is not just one more step towards more-sensitive measurements, but is a decisive jump to a more-fundamental understanding of biology<sup>41</sup>. For a long time it is assumed that cell cultures were of homogeneous nature, and analyze a collection of cells would give an accurate assessment of the behavior of the cells in that culture or tissue. This means that the average response of the cells can be interpret as the response of the all cells in that sample<sup>42</sup>. Thus, droplet microfluidics certainly plays a significant role in elucidating the heterogeneities of cell populations and their underlying causes, finding the rare cells that average only a single cell per milliliter of blood. Droplets features allow many of the challenges in single-cell analysis to be overcome<sup>43</sup>. There are of course challenges with integration as the droplet microfluidics circuitry becomes more complex, nevertheless droplet microfluidics has the potential to support scientific progress in further analysis of the fundamental component of life- the cell.

### 1.3.1.1 *Circulating tumor cells detection*

Circulating tumor cells are small amount of cells shedding into bloodstream from both primary and metastatic lesions and are thought to be responsible for the hematogenous spread of cancer to distant sites<sup>44-46</sup>. Strong evidence for CTCs as prognostic markers has been documented for breast cancer<sup>47</sup>, but CTC detection is also connected to metastatic

relapse and progression in other tumor entities, including prostate, lung and colorectal cancer<sup>48-51</sup>. In ongoing studies, the clinical utility of CTCs for treatment decisions is being evaluated<sup>51</sup>. In particular the use of CTCs as a real-time liquid biopsy has received attention during the past years<sup>52</sup>. In addition, their capture directly from a patient's blood is a non invasive method for cancer detection. However, the capture of CTCs from a patient's blood with high efficiency and purity is still a technical challenge. The capture and analysis of CTCs is very difficult owing to the low levels of these cells in blood<sup>53</sup> (approximately one CTC in a billion blood cells is seen in cancer patient blood). Moreover, the heterogeneous nature of CTCs poses an additional challenge, as there is no unique marker for their identification<sup>53-56</sup>. Furthermore, in order to carry out cell culture and molecular analysis of the CTCs, their capture are expected to be kept viable.

Various techniques have been recently explored to isolate CTCs from patient blood (figure 1.4) in which microtechnologies devices and materials have been demonstrated as possible solutions<sup>57</sup>.

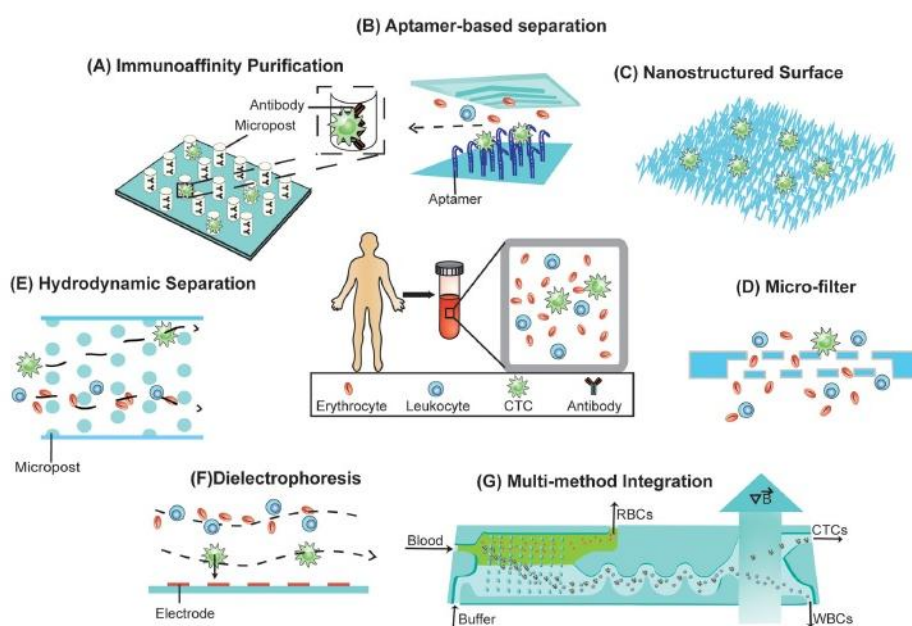


**Figure 1.4:** CTC separation methods. A) Immunoaffinity purification; B) Aptamer-based separation; C) Nanorough surfaces; D) Microfilters; E) Hydrodynamic separation; F) Dielectrophoresis; G) Approaches integrating multiple CTC capture principles together. Reproduced with permission from Ref [57]

At the moment the only system commercially available which gets approval from the US Food and Drug Administration (FDA) for CTC analysis is CellSearch. It is an immunomagnetic enrichment method that relies on targeting a marker specific to epithelial cells, the epithelial cell adhesion molecule (EpCAM). However CellSearch has a number

of limitations, for examples has a lack of sensitivity that limits its applicability to the analysis of cells with high EpCAM levels<sup>58,59</sup>, and not all CTCs present high EpCAM-expression. An additional constraint is the inability to access cellular material after cells are enumerated. To this end it is necessary develop technologies that have to be efficient enough to recover as many CTCs as possible thus ensuring the enumeration process reflects the status of the cancer patient and guarantees enough CTCs for the post-capture analysis to study the cancer metastasis process. Separation methods should be therefore able to release CTCs without damaging them and need to be less time-consuming and be able of conducting high-throughput separation, due to the short life of CTCs<sup>60</sup>. Finally, these technologies must be effective for most types of cancer patients and cancer at different disease stages.

### *1.3.2 Droplet microfluidic: a platform for functional microparticles production for detection applications.*

Droplet microfluidic techniques provide some of the most promising approaches to produce and functionalize monodisperse polymeric microparticles<sup>61</sup> for biosensing and detection (figure 1.5).

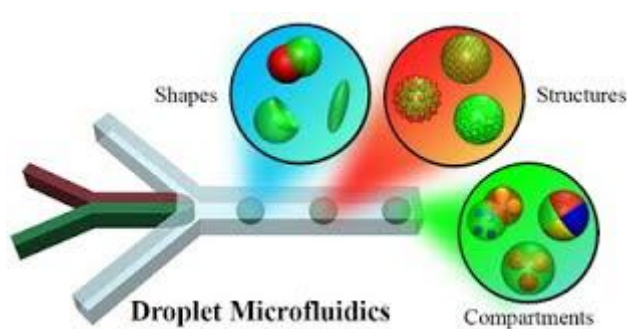


**Figure 1.5:** Functional microparticles tailored by droplet-based microfluidics. Reproduced with permission from Ref. [61]

These microparticles are obtained through the polymerization of the emulsion microdroplets template, generated by microfluidic device. Polymerization can be perform via different mechanisms: heat-based, light-based and chemical-reaction-based methods<sup>17</sup>. In all cases the discrete phases are comprised of a thermally, photochemically or chemically curable material that can be converted into solid microparticles under specific stimuli.

Polymeric microparticles can be functionalized employing creative strategies in droplet microfluidics, which are difficult to achieve using conventional suspension. For example, they can be engineered with diverse biological entities such as peptide, protein or nucleic acids<sup>62</sup> to detect proteins, DNA, mRNA, microRNA in complex fluid<sup>63</sup>.

A few reports investigated the synthesis of enzyme-immobilized hydrogel microparticles and their ability for the biosensing of small molecules<sup>64</sup>. For example, in 2012 Kantak et al. used microfluidic T-junction to generate poly(ethylene) glycol (PEG) microparticles, containing fluorescein isothiocyanate dextran (FITC-dextran) and a sugar binding protein, for a fluorescence-based glucose detection assay<sup>65</sup>.

### 1.3.2.1 Poly(ethylene glycol) (PEG) microparticles

Polyethylene glycols (PEG) (figure 1.6) are commonly used in biotechnological applications due to their biocompatibility and low-biofouling properties<sup>62,66-68</sup>. In particular, PEG layers have been used to prevent non-specific binding of protein on sensing surfaces<sup>69,70</sup>.

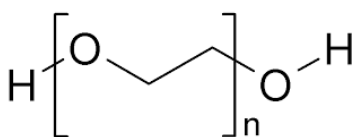


**Figure1.6:** Polyethylene glycols (PEG)

PEGs are relatively inexpensive and available in a large range of molecular weights and chemical modifications: PEG molecular weights ranging from a few hundred to several thousand grams per mole have been used to fabricate particles<sup>71</sup>. Conveniently, PEGs show good solubility in aqueous buffers required for biomolecule manipulation and PEG particles have thus been the substrate of choice for hydrogel particle-based assays so far.

PEG microparticles are usually prepared using the free-radical polymerization of reactive (meth)acrylate PEG derivatives or polyethylene glycol diacrylates (PEGDA) in the presence of a UV-sensitive photoinitiator<sup>72-74</sup>. The UV-induced activation of the photoinitiator generates a benzoyl free radical through a homolytic scission of a C–C bond, subsequently triggering the covalent crosslinking of the gel<sup>75</sup>.

One immunoassay on PEG microparticles was reported by Appleyard et al. in 2011<sup>76</sup>. The authors developed a complete sandwich immunoassay for multiplexed detection of cytokines on barcoded poly(ethilenglycol) dyacrilate (PEGDA) particles synthesized through microfluidic device. Target samples were spiked in fetal bovine serum (FBS) in

order to mimic the complexity of biological samples. The bio-inert poly PEG hydrogel did not collect non-specific signal in these complex samples, avoiding the need for prior purification of the sample.

### 1.3.2.2 Microfluidics for food analysis: aflatoxin M1

Microfluidics is a technology that allows constructing small, fast and cheap microfluidic analytical systems for food analysis<sup>77</sup>. The presence of a variety of food contaminants and residues at low concentration, their difference in physicochemical behavior and the complexity of the food matrix make food analysis a challenging task. Chromatographic techniques are commonly used in food analysis<sup>78</sup>, however they are relative slow, require extensive sample preparation and need trained personnel. As a consequence, they are expensive and time consuming for routine analysis.

The need for cheap and high throughput has encouraged the development of new technologies and more suitable analytical methods<sup>79</sup>.

In the last two decades, one of the major challenges in the field of food analysis, is the detection of aflatoxins (AFs). AFs are a major class of mycotoxins produced primarily by *Aspergillus* species<sup>80</sup>. Aflatoxin M<sub>1</sub> (AFM<sub>1</sub>) is the most toxic, carcinogenic, teratogenic and mutagenic class of AFs<sup>81</sup>; it is a hydroxylated metabolite of aflatoxin B<sub>1</sub> (AFB<sub>1</sub>) (figure 1.7) and it is normally excreted in milk by dairy mammals as a result of the direct intake of AFB<sub>1</sub>-contaminated feedstuff.

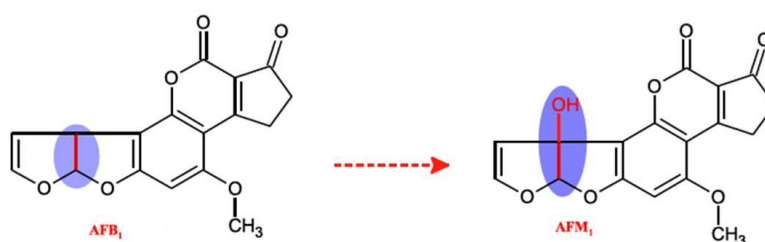


**Figure 1.7:** aflatoxin B1 metabolism

AFM<sub>1</sub> has been classified as a Group 1 carcinogenic agent by the International Agency for Research on Cancer in 2002 (IARC 2002). Once present in milk, AFM<sub>1</sub> is unaffected by thermal treatments, such as pasteurization or sterilization<sup>82</sup>. In 2006, the European Union (EU) set the legal limit for AFM<sub>1</sub> to 0.05 µg/Kg. This has prompted the adoption of regulatory limits in several countries, which, in turn, requires the development of validated official analytical methods for rapid and cost-effective screening of AFM<sub>1</sub> on a large scale. Various analytical methods and strategies have been applied for the detection of AFM<sub>1</sub>,

---

e.g., thin-layer chromatography (TLC), HPLC, gas chromatography (GC), liquid chromatography–mass spectrometry (LC-MS), enzyme-linked immunosorbent assay (ELISA), direct fluorimetry, fluorescence polarization, and various biosensors/lateral flow devices (LFD)<sup>83-88</sup>. However, it is known that these methods not only require expensive instruments and skilled operators but also complicated sample pretreatment thus limiting their application, especially in developing countries<sup>89</sup>. In this perspective, the use of droplet-based microfluidics coupled with the use of biorecognition elements (such as enzymes, peptides and antibodies) could realize simple and low cost platform for aflatoxins detection.

### ***1.4 Outline of Dissertation***

Microfluidics is an increasingly tool for single-cells analysis and also for functional gel microparticles production. We use droplet microfluidics to study rare cancer cells and to synthesize polymeric microparticles for selective protein detection in complex fluid. The final aim of this work concerns the realization and the optimization of microfluidic technologies for the development of diagnostics tools for personal care and of relative simple and rapid system for food contaminants detection.

In **Chapter 2** a microfluidics approach for circulating tumor cells (CTCs) detection, based on single-cell metabolism determination, is presented. Droplet microfluidics is used to compartmentalize each cell inside a picoliter droplet and lactic acid production by compartmentalized cancer cells is detected by monitoring the pH of the droplet through LIF at approximately 1kHz. The results are promising, and open the routs for further work in vivo.

In **Chapter 3** droplet microfluidics for functional microgels synthesis, for biosensing application, is presented. A labeled peptide was encapsulated into microparticles for specific molecules detection in complex media. The encapsulation of the peptide increase the specificity and the sensitivity of the biomolecules detection, providing an advantage in biotechnological field.

Finally, in **Chapter 4**, microfluidic microparticles for label-free AFM<sub>1</sub> detection is presented. The same method described in Chapter 3 is used for the production of functional PEGDA-microparticles for AFM<sub>1</sub> screening. Two novel peptides, synthesized in our laboratory for specific aflatoxin recognition, were encapsulated into the polymer

network. Due to AFM<sub>1</sub> natural fluorescence, the efficacy of the method was provided by CM.

Final conclusions and future perspectives, with some parameters that still need to be optimized are synthetically presented and discussed in **Chapter 5**.

---

*References*

- 1 Lederberg, J. A simple method for isolating individual microbes. *Journal of bacteriology* **68**, 258 (1954).
- 2 Theberge, A. B. *et al.* Microdroplets in microfluidics: an evolving platform for discoveries in chemistry and biology. *Angewandte Chemie International Edition* **49**, 5846-5868 (2010).
- 3 Whitesides, G. M. The origins and the future of microfluidics. *Nature* **442**, 368-373 (2006).
- 4 Manz, A., Graber, N. & Widmer, H. á. Miniaturized total chemical analysis systems: a novel concept for chemical sensing. *Sensors and actuators B: Chemical* **1**, 244-248 (1990).
- 5 Reyes, D. R., Iossifidis, D., Auroux, P.-A. & Manz, A. Micro total analysis systems. 1. Introduction, theory, and technology. *Analytical chemistry* **74**, 2623-2636 (2002).
- 6 Song, H. & Ismagilov, R. F. Millisecond kinetics on a microfluidic chip using nanoliters of reagents. *Journal of the American Chemical Society* **125**, 14613-14619 (2003).
- 7 Zheng, B., Tice, J. D., Roach, L. S. & Ismagilov, R. F. A Droplet-Based, Composite PDMS/Glass Capillary Microfluidic System for Evaluating Protein Crystallization Conditions by Microbatch and Vapor-Diffusion Methods with On-Chip X-Ray Diffraction. *Angewandte chemie international edition* **43**, 2508-2511 (2004).
- 8 Tice, J. D., Song, H., Lyon, A. D. & Ismagilov, R. F. Formation of droplets and mixing in multiphase microfluidics at low values of the Reynolds and the capillary numbers. *Langmuir* **19**, 9127-9133 (2003).
- 9 Thorsen, T., Roberts, R. W., Arnold, F. H. & Quake, S. R. Dynamic pattern formation in a vesicle-generating microfluidic device. *Physical review letters* **86**, 4163 (2001).
- 10 Umbanhowar, P., Prasad, V. & Weitz, D. Monodisperse emulsion generation via drop break off in a coflowing stream. *Langmuir* **16**, 347-351 (2000).
- 11 Mazutis, L. *et al.* Droplet-based microfluidic systems for high-throughput single DNA molecule isothermal amplification and analysis. *Analytical chemistry* **81**, 4813-4821 (2009).

- 
- 12 Zheng, B., Roach, L. S. & Ismagilov, R. F. Screening of protein crystallization conditions on a microfluidic chip using nanoliter-size droplets. *Journal of the American chemical society* **125**, 11170-11171 (2003).
  - 13 Cho, S. K., Moon, H. & Kim, C.-J. Creating, transporting, cutting, and merging liquid droplets by electrowetting-based actuation for digital microfluidic circuits. *Microelectromechanical Systems, Journal of* **12**, 70-80 (2003).
  - 14 Cai, L., Friedman, N. & Xie, X. S. Stochastic protein expression in individual cells at the single molecule level. *Nature* **440**, 358-362 (2006).
  - 15 Leng, J. & Salmon, J.-B. Microfluidic crystallization. *Lab on a Chip* **9**, 24-34 (2009).
  - 16 Guo, M. T., Rotem, A., Heyman, J. A. & Weitz, D. A. Droplet microfluidics for high-throughput biological assays. *Lab on a Chip* **12**, 2146-2155 (2012).
  - 17 Dendukuri, D. & Doyle, P. S. The synthesis and assembly of polymeric microparticles using microfluidics. *Advanced Materials* **21**, 4071-4086 (2009).
  - 18 Fair, R. B. Digital microfluidics: is a true lab-on-a-chip possible? *Microfluidics and Nanofluidics* **3**, 245-281 (2007).
  - 19 Link, D. R. *et al.* Electric control of droplets in microfluidic devices. *Angewandte Chemie International Edition* **45**, 2556-2560 (2006).
  - 20 Teh, S.-Y., Lin, R., Hung, L.-H. & Lee, A. P. Droplet microfluidics. *Lab on a Chip* **8**, 198-220 (2008).
  - 21 Ahmed, R. & Jones, T. Dispensing picoliter droplets on substrates using dielectrophoresis. *Journal of electrostatics* **64**, 543-549 (2006).
  - 22 Roux, J.-M., Fouillet, Y. & Achard, J.-L. 3D droplet displacement in microfluidic systems by electrostatic actuation. *Sensors and Actuators A: Physical* **134**, 486-493 (2007).
  - 23 Gu, H., Duits, M. H. & Mugele, F. Droplets formation and merging in two-phase flow microfluidics. *International journal of molecular sciences* **12**, 2572-2597 (2011).
  - 24 Engl, W., Backov, R. & Panizza, P. Controlled production of emulsions and particles by milli-and microfluidic techniques. *Current Opinion in Colloid & Interface Science* **13**, 206-216 (2008).
  - 25 Shepherd, R. F. *et al.* Microfluidic assembly of homogeneous and janus colloid-filled hydrogel granules. *Langmuir* **22**, 8618-8622 (2006).
  - 26 Baroud, C. N., Gallaire, F. & Danga, R. Dynamics of microfluidic droplets. *Lab on a Chip* **10**, 2032-2045 (2010).

- 
- 27 Kiss, M. M. *et al.* High-throughput quantitative polymerase chain reaction in picoliter droplets. *Analytical chemistry* **80**, 8975-8981 (2008).
- 28 Barbulovic-Nad, I., Yang, H., Park, P. S. & Wheeler, A. R. Digital microfluidics for cell-based assays. *Lab on a Chip* **8**, 519-526 (2008).
- 29 Srinivasan, V., Pamula, V. K. & Fair, R. B. Droplet-based microfluidic lab-on-a-chip for glucose detection. *Analytica Chimica Acta* **507**, 145-150 (2004).
- 30 Dittrich, P. S. & Manz, A. Lab-on-a-chip: microfluidics in drug discovery. *Nature Reviews Drug Discovery* **5**, 210-218 (2006).
- 31 i Solvas, X. Droplet microfluidics: recent developments and future applications. *Chemical Communications* **47**, 1936-1942 (2011).
- 32 Joensson, H. N. & Andersson Svahn, H. Droplet Microfluidics—A Tool for Single-Cell Analysis. *Angewandte Chemie International Edition* **51**, 12176-12192 (2012).
- 33 Lindström, S. & Andersson-Svahn, H. Overview of single-cell analyses: microdevices and applications. *Lab on a Chip* **10**, 3363-3372 (2010).
- 34 Chabert, M., Dorfman, K. D. & Viovy, J. L. Droplet fusion by alternating current (AC) field electrocoalescence in microchannels. *Electrophoresis* **26**, 3706-3715 (2005).
- 35 Link, D., Anna, S. L., Weitz, D. & Stone, H. Geometrically mediated breakup of drops in microfluidic devices. *Physical review letters* **92**, 054503 (2004).
- 36 Ahn, K. *et al.* Dielectrophoretic manipulation of drops for high-speed microfluidic sorting devices. *Applied Physics Letters* **88**, 24104-24104 (2006).
- 37 Baret, J.-C. *et al.* Fluorescence-activated droplet sorting (FADS): efficient microfluidic cell sorting based on enzymatic activity. *Lab on a Chip* **9**, 1850-1858 (2009).
- 38 Agresti, J. *et al.* Ultrahigh-throughput screening in drop-based microfluidics for directed evolution. *Proc Natl Acad Sci USA* **107**, 6550 (2010).
- 39 Huebner, A. *et al.* Development of quantitative cell-based enzyme assays in microdroplets. *Analytical chemistry* **80**, 3890-3896 (2008).
- 40 Mazutis, L. *et al.* Single-cell analysis and sorting using droplet-based microfluidics. *Nature protocols* **8**, 870-891 (2013).
- 41 Seok, J. *et al.* Genomic responses in mouse models poorly mimic human inflammatory diseases. *Proceedings of the National Academy of Sciences* **110**, 3507-3512 (2013).
- 42 Schmid, A., Kortmann, H., Dittrich, P. S. & Blank, L. M. Chemical and biological single cell analysis. *Current opinion in biotechnology* **21**, 12-20 (2010).

- 
- 43 Brouzes, E. *et al.* Droplet microfluidic technology for single-cell high-throughput screening. *Proceedings of the National Academy of Sciences* **106**, 14195-14200 (2009).
- 44 O'Flaherty, J. D. *et al.* Circulating tumour cells, their role in metastasis and their clinical utility in lung cancer. *Lung Cancer* **76**, 19-25 (2012).
- 45 Plaks, V., Koopman, C. D. & Werb, Z. Circulating tumor cells. *Science (New York, NY)* **341** (2013).
- 46 Conteduca, V. *et al.* Circulating tumor cells: utopia or reality? *Future Oncology* **9**, 1337-1352 (2013).
- 47 Cristofanilli, M. *et al.* Circulating tumor cells, disease progression, and survival in metastatic breast cancer. *New England Journal of Medicine* **351**, 781-791 (2004).
- 48 Scher, H. I. *et al.* Circulating tumour cells as prognostic markers in progressive, castration-resistant prostate cancer: a reanalysis of IMMC38 trial data. *The lancet oncology* **10**, 233-239 (2009).
- 49 Hou, J.-M. *et al.* Clinical significance and molecular characteristics of circulating tumor cells and circulating tumor microemboli in patients with small-cell lung cancer. *Journal of Clinical Oncology* **30**, 525-532 (2012).
- 50 Aggarwal, C. *et al.* Relationship among circulating tumor cells, CEA and overall survival in patients with metastatic colorectal cancer. *Annals of oncology* **24**, 420-428 (2013).
- 51 Bidard, F.-C. *et al.* Clinical application of circulating tumor cells in breast cancer: overview of the current interventional trials. *Cancer and Metastasis Reviews* **32**, 179-188 (2013).
- 52 Pantel, K. & Alix-Panabières, C. Real-time liquid biopsy in cancer patients: fact or fiction? *Cancer research* **73**, 6384-6388 (2013).
- 53 den Toonder, J. Circulating tumor cells: the Grand Challenge. *Lab on a chip* **11**, 375-377 (2011).
- 54 Gasch, C. *et al.* Heterogeneity of epidermal growth factor receptor status and mutations of KRAS/PIK3CA in circulating tumor cells of patients with colorectal cancer. *Clinical chemistry* **59**, 252-260 (2013).
- 55 Bednarz-Knoll, N., Alix-Panabières, C. & Pantel, K. Plasticity of disseminating cancer cells in patients with epithelial malignancies. *Cancer and Metastasis Reviews* **31**, 673-687 (2012).

- 
- 56 Willipinski-Stapelfeldt, B. *et al.* Changes in cytoskeletal protein composition indicative of an epithelial-mesenchymal transition in human micrometastatic and primary breast carcinoma cells. *Clinical Cancer Research* **11**, 8006-8014 (2005).
- 57 Qian, W., Zhang, Y. & Chen, W. Capturing Cancer: Emerging Microfluidic Technologies for the Capture and Characterization of Circulating Tumor Cells. *Small* (2015).
- 58 Sieuwerts, A. M. *et al.* Anti-epithelial cell adhesion molecule antibodies and the detection of circulating normal-like breast tumor cells. *Journal of the National Cancer Institute* **101**, 61-66 (2009).
- 59 Farace, F. *et al.* A direct comparison of CellSearch and ISET for circulating tumour-cell detection in patients with metastatic carcinomas. *British journal of cancer* **105**, 847-853 (2011).
- 60 Pantel, K., Alix-Panabières, C. & Riethdorf, S. Cancer micrometastases. *Nature reviews Clinical oncology* **6**, 339-351 (2009).
- 61 Kim, J. H. *et al.* Droplet microfluidics for producing functional microparticles. *Langmuir* **30**, 1473-1488 (2013).
- 62 Peppas, N. A., Hilt, J. Z., Khademhosseini, A. & Langer, R. Hydrogels in biology and medicine: from molecular principles to bionanotechnology. *ADVANCED MATERIALS-DEERFIELD BEACH THEN WEINHEIM-* **18**, 1345 (2006).
- 63 Helgeson, M. E., Chapin, S. C. & Doyle, P. S. Hydrogel microparticles from lithographic processes: Novel materials for fundamental and applied colloid science. *Current opinion in colloid & interface science* **16**, 106-117 (2011).
- 64 Zhu, Q. & Trau, D. Multiplex detection platform for tumor markers and glucose in serum based on a microfluidic microparticle array. *Analytica chimica acta* **751**, 146-154 (2012).
- 65 Kantak, C., Zhu, Q., Beyer, S., Bansal, T. & Trau, D. Utilizing microfluidics to synthesize polyethylene glycol microbeads for Förster resonance energy transfer based glucose sensing. *Biomicrofluidics* **6**, 022006 (2012).
- 66 Langer, R. & Tirrell, D. A. Designing materials for biology and medicine. *Nature* **428**, 487-492 (2004).
- 67 Peppas, N. A., Keys, K. B., Torres-Lugo, M. & Lowman, A. M. Poly (ethylene glycol)-containing hydrogels in drug delivery. *Journal of controlled release* **62**, 81-87 (1999).

- 
- 68 Nguyen, K. T. & West, J. L. Photopolymerizable hydrogels for tissue engineering applications. *Biomaterials* **23**, 4307-4314 (2002).
- 69 Lin, Z. *et al.* An extremely simple method for fabricating 3D protein microarrays with an anti-fouling background and high protein capacity. *Lab on a Chip* **14**, 2505-2514 (2014).
- 70 Hucknall, A., Rangarajan, S. & Chilkoti, A. In pursuit of zero: polymer brushes that resist the adsorption of proteins. *Advanced Materials* **21**, 2441-2446 (2009).
- 71 Ren, Y. M. *et al.* in *Advanced Materials Research*. 178-181 (Trans Tech Publ).
- 72 Meiring, J. E. *et al.* Hydrogel biosensor array platform indexed by shape. *Chemistry of materials* **16**, 5574-5580 (2004).
- 73 Park, S. *et al.* Entrapment of enzyme-linked magnetic nanoparticles within poly (ethylene glycol) hydrogel microparticles prepared by photopatterning. *Reactive and Functional Polymers* **69**, 293-299 (2009).
- 74 Lewis, C. L., Choi, C.-H., Lin, Y., Lee, C.-S. & Yi, H. Fabrication of uniform DNA-conjugated hydrogel microparticles via replica molding for facile nucleic acid hybridization assays. *Analytical chemistry* **82**, 5851-5858 (2010).
- 75 Andrzejewska, E. Photopolymerization kinetics of multifunctional monomers. *Progress in polymer science* **26**, 605-665 (2001).
- 76 Appleyard, D. C., Chapin, S. C., Srinivas, R. L. & Doyle, P. S. Bar-coded hydrogel microparticles for protein detection: synthesis, assay and scanning. *Nature protocols* **6**, 1761-1774 (2011).
- 77 Atalay, Y. T. *et al.* Microfluidic analytical systems for food analysis. *Trends in food science & technology* **22**, 386-404 (2011).
- 78 Lehotay, S. J. & Hajšlová, J. Application of gas chromatography in food analysis. *TrAC Trends in Analytical Chemistry* **21**, 686-697 (2002).
- 79 Asensio-Ramos, M., Hernández-Borges, J., Rocco, A. & Fanali, S. Food analysis: a continuous challenge for miniaturized separation techniques. *Journal of separation science* **32**, 3764-3800 (2009).
- 80 Creppy, E. E. Update of survey, regulation and toxic effects of mycotoxins in Europe. *Toxicology letters* **127**, 19-28 (2002).
- 81 Iqbal, S. Z. *et al.* Aflatoxin B1 in chilies from the Punjab region, Pakistan. *Mycotoxin research* **26**, 205-209 (2010).
- 82 Galvano, F. *et al.* Survey of the occurrence of aflatoxin M1 in dairy products marketed in Italy. *Journal of Food Protection*® **61**, 738-741 (1998).

- 
- 83 Tang, D., Liu, B., Niessner, R., Li, P. & Knopp, D. Target-induced displacement reaction accompanying cargo release from magnetic mesoporous silica nanocontainers for fluorescence immunoassay. *Analytical chemistry* **85**, 10589-10596 (2013).
- 84 Wang, Y. *et al.* Isolation of alpaca anti-idiotypic heavy-chain single-domain antibody for the aflatoxin immunoassay. *Analytical chemistry* **85**, 8298-8303 (2013).
- 85 Li, X. *et al.* Molecular characterization of monoclonal antibodies against aflatoxins: a possible explanation for the highest sensitivity. *Analytical chemistry* **84**, 5229-5235 (2012).
- 86 Parker, C. O., Lanyon, Y. H., Manning, M., Arrigan, D. W. & Tothill, I. E. Electrochemical immunochip sensor for aflatoxin M1 detection. *Analytical chemistry* **81**, 5291-5298 (2009).
- 87 He, T. *et al.* Nanobody-based enzyme immunoassay for aflatoxin in agro-products with high tolerance to cosolvent methanol. *Analytical chemistry* **86**, 8873-8880 (2014).
- 88 Wang, Y. *et al.* Phage-displayed peptide that mimics aflatoxins and its application in immunoassay. *Journal of agricultural and food chemistry* **61**, 2426-2433 (2013).
- 89 Iqbal, S. Z., Jinap, S., Pirouz, A. & Faizal, A. A. Aflatoxin M 1 in milk and dairy products, occurrence and recent challenges: A review. *Trends in Food Science & Technology* **46**, 110-119 (2015).

### *A microfluidic approach for single-cell metabolism determination, a tool for circulating tumor cells detection*

**Abstract.** The number of circulating tumor cells (CTCs) in blood is strongly correlated with the progress of metastatic cancer, for this reason their capture and retain represents a major challenge in cancer research. Traditional methods to isolate and characterize CTCs are based on immunostaining or discrimination of physical properties. Recently microengineered devices have been demonstrated as a possible solution to capture and processing of CTCs. Here, a label-free method is presented. It exploits the so-called Warburg effect (WE): even in the presence of oxygen cancer cells limit largely their metabolism to glycolysis leading to increased production of lactate. Cells are compartmentalized into a pL droplets using droplet microfluidics. Cancer cells secrete lactic acid faster than healthy cells, acidifying the extracellular environment. The lactic acid production can be detect by monitoring the pH changes within droplets. Cancer cells are detected by finding droplets with significant pH changes. This method is capable of retrieving live cells, opening up routes for further large scale investigation of the nature of CTCs.

This work has partly been submitted for publication: Fabio Del Ben<sup>†\*</sup>, Matteo Turetta<sup>†</sup>, Giorgia Celetti, Aigars Piruska, Michela Bulfoni, Daniela Cesselli, Wilhelm T.S. Huck\*, Giacinto Scoles\* “**A microfluidic approach to single-cell metabolism determination, as a basis for circulating tumor cells detection**”

---

## 2.1. Introduction

The progression of cancer from a localized tumor to metastasis is central to often devastating effects of this complex illness. A release of CTCs from primary tumor into the bloodstream is one of main routes for the formation of metastases in distant organs<sup>1</sup>. CTCs that possess an aggressive phenotype can invade a healthy tissue and form secondary tumors, which are often cause of patient's death. A recent clinical research has shown that level of CTCs in metastatic patient's blood is a predictor of survival, indicating the value of CTCs as a biomarker for cancer diagnosis, prognostic outcome evaluation, and treatment monitoring<sup>2-5</sup>. Therefore, the isolation and the analysis of CTCs has a potential to provide an insight in blood-born metastasis and monitor cancer response noninvasively following therapeutic intervention.

The capture and analysis of CTCs is very challenging owing to their extreme rarity relative to erythrocytes ( $5 \times 10^9$  cells/mL) and leucocytes ( $7 \times 10^6$  cells/mL) in patient's blood<sup>6</sup>. Although red blood cells can be easily removed by lysis, leucocytes (white blood cells) share many of the physical, chemical and biological properties of CTCs, leading to high contamination levels in many CTC detection methods<sup>7</sup>. The heterogeneity of CTCs poses an additional challenge, as there is no unique biologic marker for their identification<sup>8,9</sup>. Biochemical techniques for detection and enumeration of CTCs exploit the presence of surface and cytoplasmic proteins (epithelial cell adhesion molecule (EpCAM), HER2, EGFR, MUC1, or CKs) that are not present in leukocytes<sup>10</sup>. Currently the only clinically validated method (CellSearch®) is based on the enumeration of epithelial cells that are separated from the blood by EpCAM-coated magnetic beads and identified with the use of fluorescently labelled antibodies against cytokeratin (8, 18, 19) and with a fluorescent nuclear stain<sup>11</sup>. CellSearch® and other methods based on immunostaining are able to detect reliably EpCAM-positive CTCs. However, a potential problem for detection of EpCAM positive CTCs is the variation of EpCAM expression in cancer cells. When detached from the primary tumor, metastatic tumor cells may experience the epithelial-to-mesenchymal transition (EMT), which leads to the disappearance of epithelial features such as EpCAM expression, and such approaches using the EpCAM biomarker may result in the loss of partial populations of CTCs, which may have more aggressive metastatic potentials<sup>12,13</sup>. To overcome this limitation alternative methods based on physical properties such as the mechanical properties of CTCs, size, deformability, or electric charge, have been

---

developed. They are low cost, label-free and, most importantly, permit significantly higher throughput compared to immunostaining-based methods. While these techniques achieved satisfactory isolation efficiency, the viability of the captured CTCs was compromised. Moreover, morphological analysis of CTCs has shown that the size of these cells varying from 4 to 30  $\mu\text{m}$ , thus some CTCs could be as large as leukocytes, resulting in a potential loss of subpopulations of CTCs<sup>14</sup>.

Although significant progress for CTCs detection has been made, further improvement is necessary. Methods capable of detection and isolation of live, intact CTCs will open opportunities for detailed analysis of CTCs and metastasis.

In the 1920s Otto Warburg observed an anomalous metabolism of cancer cells for the first time<sup>15</sup>. Even in the presence of oxygen cancer cells limit largely their metabolism to glycolysis leading to increased production of lactate, phenomenon that has been termed “Warburg effect” or “aerobic glycolysis”<sup>16</sup>. An altered metabolism of cancer cells (and associated extracellular acidification via various mechanisms) is widespread across different types of cancers, and it has been accepted as a hallmark of cancer<sup>17</sup>. The Warburg-correlated upregulation of glucose uptake is well-known, and forms the basis of F-fluorodeoxyglucose Positron-Emission Tomography (FDG-PET), currently applied in the diagnosis, staging and monitoring of almost all types of cancer<sup>18</sup>. Although the Warburg effect has been known for over 50 years, it has never been used to detect CTCs, as such cells are so rare that they do not noticeably alter lactate levels in blood.

Here we present a label-free method for CTCs detection exploiting the abnormal metabolic behavior of cancer cells (WE) using droplet microfluidics. A suspension of tumor cells from a cancer cell line (lung - A549) were emulsified in 35  $\mu\text{L}$  droplets. All molecules secreted by cancer cell are retained in the droplet and concentration of secretion product rapidly increases due to the small volume of the droplets. Thus CTCs are detected by measuring lactate or pH changes in the extracellular compartment without the need for surface-antigen labeling. We then mixed A549 cells with white blood cells (WBCs), as these will be the primary background in blood samples taken from patients, and observed a clear  $\sim 2$  fold intensity difference between droplets containing cancer cells and empty or WBC containing drops (**Figure 2.1**).

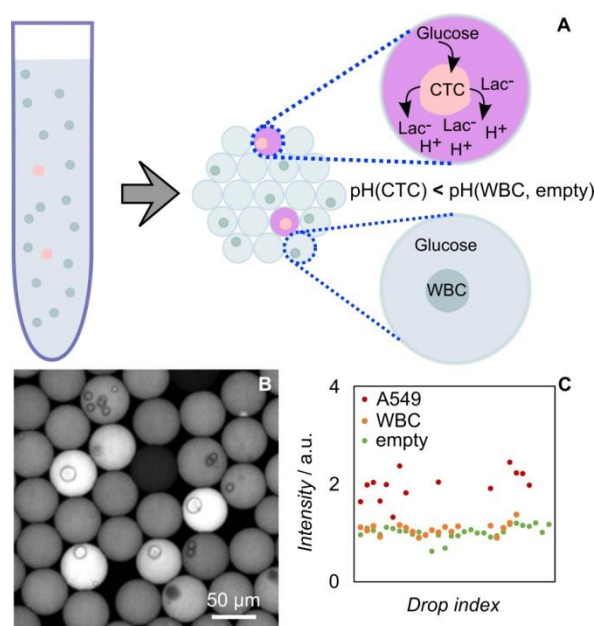


**Figure 2.1:** schematic representation. A) lactate secretion by CTCs provide an acidification of extracellular environment; B) different of fluorescent between droplets contain cancer cells and empty or WBC containing drops; C) detection of environment acidification due to lactate secretion via pH measurement.

## 2.2. Results and discussion

### 2.2.1. Characterization using cell lines

The key technological breakthrough presented here lies in splitting the macroscopic (blood) sample into small (picoliter-nanoliter) aqueous droplets in oil (water-in-oil emulsion) using droplet microfluidics<sup>19</sup>. Each droplet contains at most a single cell and all molecules secreted by this single cell are retained by the droplet<sup>20</sup>. To establish the validity of our approach, we emulsified a suspension of tumor cells from a cancer cell line (lung - A549) in 35 pL droplets in the presence of culture medium and a lactic acid assay mixture. The number of cells in each droplet followed a Poisson distribution ensuring >90% single cell encapsulation (**Figure 2.2**) and we demonstrated the production of lactate by A549 in drops.

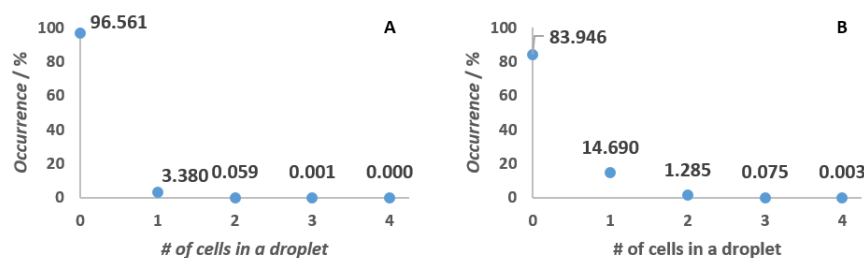


**Figure 2.2:** distribution of cell occupancy in droplets. Distributions shown for emulsification of 1 000 000 cell/mL (A) and 5 000 000 cell/mL (B). By far the majority of droplets are empty, but more than 90% of droplets containing cells have only 1 cell per droplet.

In order to simplify the assay, we measured lactate secretion indirectly, by monitoring the pH of the droplet using a ratiometric pH-sensitive dye (Snarf-5F). **Figure 2.3** clearly show a difference in fluorescent intensity, that means a drop in pH inside droplets, between empty droplets, droplets containing cancer cells or containing WBCs. There is some spread in the fluorescence. This variation is most likely due to a difference in lactate secretion rates between individual cells.

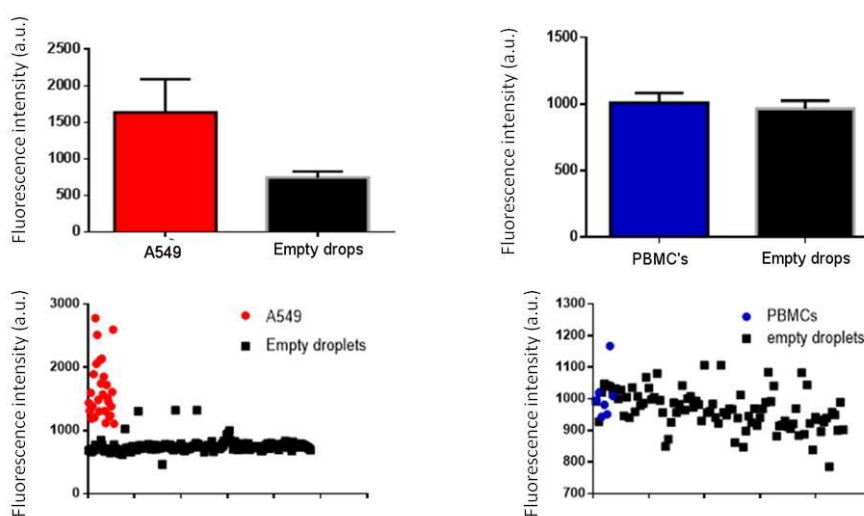


**Figure 2.3:** detection of acidification due to lactate secretion via pH measurement. pHrodo Green dye was used to indicate pH changes. Results are comparable to lactate assay and confirm the difference between cancer cells and WBCs.

To screen droplets with higher throughput in a semi-automated way, we engineered an inverted microscope, so that each droplet can be analyzed using laser-induced fluorescence at approximately 1 kHz<sup>21,22</sup> (**Figure 2.4**). For each droplet the ratio of emitted fluorescence at 580 and 630 nm is calculated in real time. In the presence of cell secreting lactate the pH

inside a droplet reduces below 7.4 and as a result an increase in 580/630 ratio above 1 is observed (**Figure 2.4A**).

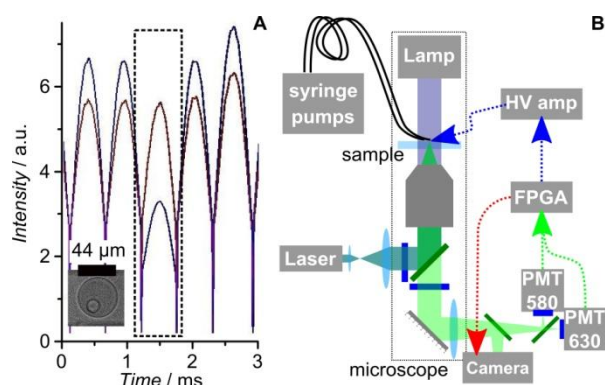


**Figure 2.4:** Detection of CTC using dual emission SNARF 5F dye. (A) Fragment of a raw data trace. Inset shows micrograph of a detected CTC. (B) Schematic of experimental setup.: laser-induced fluorescence setup.

Real time analysis of each droplet enables us to capture images (**Figure 2.4A**) of a subset of droplets with increased 580/630 fluorescence ratios, thus providing an additional verification. The assay consists of three steps: a sample emulsification, incubation and a readout. To facilitate subsequent reinjection step droplets were generated, collected and incubated in a device with a cone-shaped chamber. After incubation all droplets are injected in another device where each droplet is interrogated and fluorescence ratio is determined.

We made a calibration curve of Snarf-5f to correlate fluorescence intensity (ratio between fluorescence intensity at 580 nm and intensity at 630 nm) with pH changes inside droplets (**Figure 2.5**). A set of Joklik's modified EMEM solutions was prepared and titrated to various pHs between 7.4 and 5. These solutions were emulsified and ratio of obtained droplets detected similarly to A549 samples.

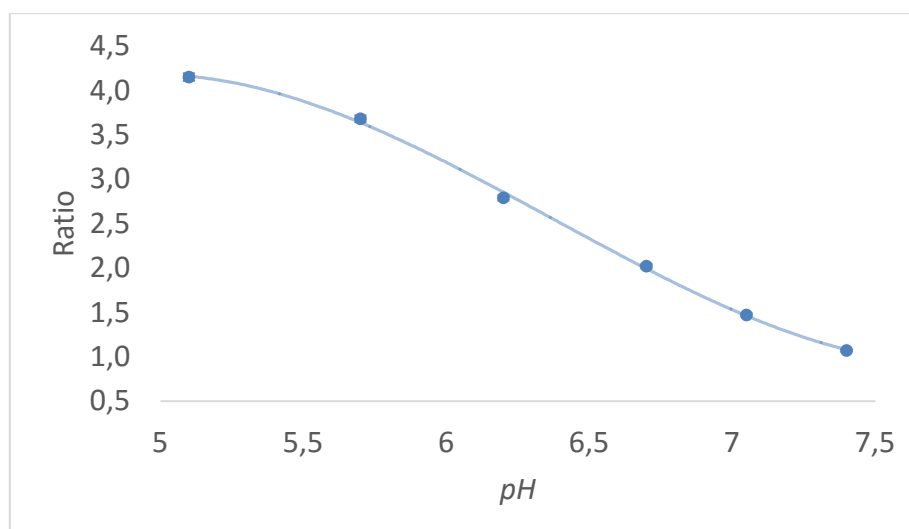


**Figure 2.5:** calibration of SNARF-5F response. Ratio between fluorescence intensity at 580 nm and intensity at 630 nm.

### 2.2.2. Outperforming other methods

Using the developed method, we investigated secretion in various cancer cell lines. The secretion of lactate leads to a rapid increase in the concentration of acid in cell-containing droplets. Even after short incubation times (<2 minutes) a population of acidified droplets appears. This population increases further, approaching saturation after 10-20 minutes. Therefore, all our experiments were carried out using incubation times of at least 10 minutes (**Figure 2.6**).

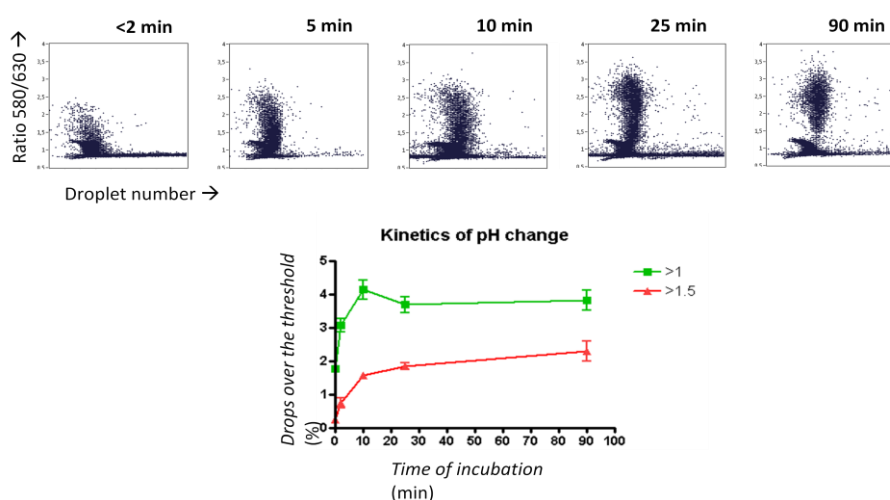


**Figure 2.6:** (Top panels) Dot plots showing a population of droplets becoming increasingly acid over time. (Bottom panel) A fraction of droplets reaching certain ratio (>1 – green trace; >1.5 – red trace)

To demonstrate that this is a general method for detection of cancer cells, we tested several other cancer cell lines, both EpCAM(+) and (-) including ovarian TOV21G, breast MDA-MB 453, glioblastoma U231, colorectal HT-29, breast MCF-7 and MDA-MB-231 - and found that all show acidification of droplets (**Figure 2.7**). The results makes our method suited to study a range of cancer types. These include epithelial cancers in which activation of EMT during cancer cell invasion triggers loss of epithelial markers, as well as non-epithelial cancers such as melanoma.

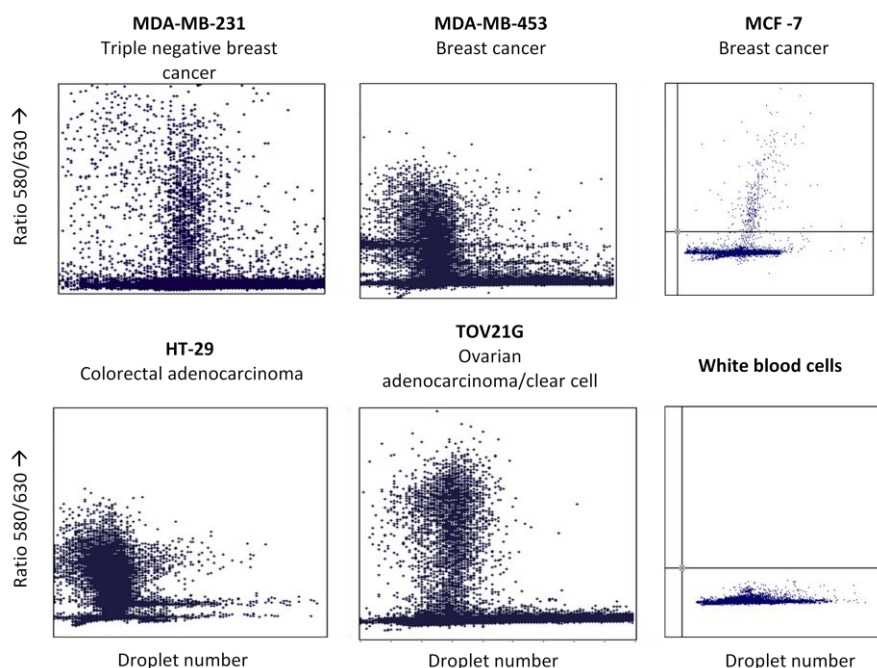


**Figure 2.7:** metabolic response of selected cancer cell lines. WBC response is given for comparison.

### 2.2.3. Optimization: A549 mixed to WBC for clinical samples simulation

We used A549 cell line mixed with WBCs to simulate clinical samples and to investigate analytical figures of merit of the developed method. Experiments were then repeated using larger numbers of cells. **Figure 2.8A** shows data points for 2 millions droplets of an emulsified A549 suspension, and we see a clear fraction of droplets with a reduced pH. **Figure 2.8B** shows data points for 2 millions droplets produced from a sample of WBCs from a healthy donor; visual inspection of the captured image of the few acidic droplets detected never confirmed the presence of WBCs. **Figure 2.8C** shows data points for 2 millions droplets of the same sample with A549 cells spiked in, leading to a distinct

population of acidified droplets. These figures clearly demonstrate that our method is capable of distinguishing healthy cells from metabolically active A549.

CTCs are extremely rare cells and the detection of these cells requires an assay with high sensitivity and specificity. To quantify both, we emulsified mixtures of A549 tumor cells with WBCs in ratios ranging from as few as 10 : 200,000 to 130 : 200,000 A549:WBC (total samples sizes containing 1M/mL WBCs). **Figure 2.8D** shows the number of tumor cells detected vs. number of tumor cells spiked in. Our method is capable of detecting A549's even at the lowest dilutions tested, with average detection rates for all experiments in the range of 60%. We note that at low cell count, deviations between expected and recovered cell numbers might be due to variations in actual cells compartmentalized, and losses due to adhesion to tubing or syringe. Importantly, none of the low pH droplets contained WBCs (as confirmed by analyzing the video images).

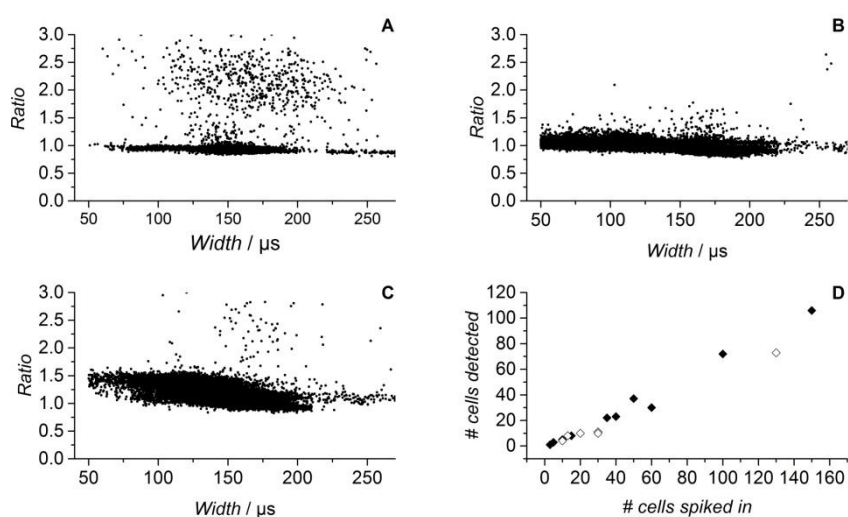


**Figure 2.8:** Detection of A549 cells. (A) A 549s alone in Joklik medium (pH 7.3). (B) isolated WBC alone in medium. (C) Mixture of A549 and WBCs in medium. (D) Absolute and relative recovery of spiked A549 in presence of WBC.

#### 2.2.4. *Capture of cancer cells from blood sample of patients*

With the method established, we tested samples based on blood of healthy donors as well as cancer patients with confirmed metastatic disease. To be able to process a large amount of blood, we depleted lysed blood of CD45+ cells by magnetic labeling (Miltenyi Biotec). **Figure 2.9** shows clearly that, in the CD45(-) fraction, no positive droplets are observed in samples derived from the blood of healthy volunteers, whereas numerous positive droplets

are detected when either A549s are spiked into the healthy donor sample, or the sample of a metastatic patient is analyzed.

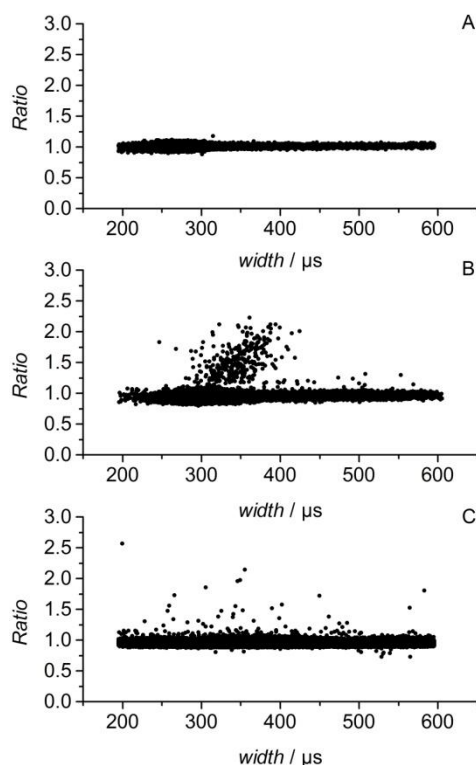


**Figure 2.9:** CTC detection in clinical samples. (A) Healthy volunteer sample. (B) Healthy volunteer sample with spiked tumor cells. (C) Sample from metastatic colorectal cancer patient.

### 2.3. Conclusions

This work provides the first proof-of-concept data that the cancer cell metabolism, and more specifically, the acidification of the extracellular microenvironment (so-called Warburg effect), can be used to identify and count rare tumor cells and CTCs. This method could overcome some limits of other technologies used for CTCs capture. Further work is needed to confirm these results and clarify how they can impact in clinical routine: positive events need to be isolated and characterized for cancer-specific proteins and genetic mutations, while clinical parameters as sensitivity, specificity, predictive values, must be established by dedicated clinical trials.

---

## *Acknowledgments*

The experimental work in this chapter was carried out together with Aigars Apiruska. Fabio del Ben and Matteo Turetta are acknowledged for patient experiments and fruitful discussion. Florian Wimmers is gratefully acknowledged for providing WBC samples.

### *2.4. Experimental Section*

*Microfluidic circuit fabrication:* 25  $\mu\text{m}$  thick layer of SU8-2025 was spun on silicon wafer, baked, exposed through transparency mask, baked again and developed according to manufacturer instructions (MicroChem corp.). Sylgard 184 (PDMS) prepolymer and crosslinking agent (Dow Corning) were mixed at a mass ratio of 10:1 (w/w); a mixture was poured onto a master, degassed and cured at 65°C for at least 2h. The replica was detached from master and reservoirs were bored using a blunt hypodermic needle. A PDMS replica was washed in soapy water and ethanol, and blow dried with nitrogen. A clean glass slide and a clean PDMS replica were treated with oxygen plasma and bonded. The device was silanized with 1% (Tridecafluoro-1,1,2,2-Tetrahydrooctyl)-1-Trichlorosilane (Sigma-Aldrich) in FC-40 (3M), fluorinated oil, which was introduced into microfluidic channels (enough to completely wet whole microfluidic network) and then the device was kept at 95°C for at least 30 min. To fabricate a reservoir for an emulsified sample a brass cone (10 mm in dia. and 5 mm tall; ~130  $\mu\text{L}$  volume) was placed directly on silicon wafer and replicated together with photolithographically defined features.

*Cells:* Cell lines were a courtesy of Di Loreto lab, Hubrecht lab, and Colombatti lab. White blood cells (WBCs) were obtained by lysing whole blood with lysis solution (BD) according to manufacturer's protocol.

*Droplet production:* Monodisperse droplets are generated in chips with 20  $\mu\text{m}$  wide T-junction. Continuous phase: 2% (w/w) surfactant (Krytox–Jeffamine–Krytox A–B–A triblock copolymer)<sup>1</sup> in HFE-7500 (3M) Dispersed phase: cell suspension in HBSS or Joklik's modified EMEM, Optiprep 15%, pH-sensitive dye (4  $\mu\text{M}$ ). Flow rates are set such

---

<sup>1</sup> V.Chokkalingam, J.Tel, F.Wimmers, X.Liu, S.Semenov, J.Thiele, C.G.Figdor, W.T.S.Huck, *Lab Chip* **2013**,*13*, 4740-4744, doi: 10.1039/C3LC50945A

---

as continuous phase flow is at least 2 times higher than a flow rate of a dispersed phase; a typical flow rate for dispersed phase was 300  $\mu\text{l/h}$  and 600  $\mu\text{l/h}$  for continuous phase.

*Lactate enzymatic assay:* A three-channel architecture microfluidic circuit was used: one channel bringing the cell suspension (dispersed phase), one bringing the reagents of lactate assay (Cell Technology, Inc.) and one bringing continuous phase. Emulsification step was performed at 4°C to slow down cell metabolism to avoid lactate contamination of the whole solution by cancer cells. With this microfluidic device we could expose cells to the enzymes of the lactate assay only after encapsulation in the micro-droplets, to avoid unspecific activation prior the encapsulation. Images were taken after 15 min incubation at room temperature after emulsification.

*Widefield fluorescence imaging* (lactate assay, pHRedo green experiments): An inverted epifluorescence microscope (Olympus IX81) was equipped with xCite 120Q lamp (Lumen Dynamics Group Inc.), resorufin and FITC filter sets (Semrock) and iXon 897 camera (Andor). An aliquot of processed sample was pipetted on a microscope glass slide and covered with a cover slip to prevent evaporation.

*High throughput detection with SNARF-5F. Setup:* An inverted microscope (Olympus IX70) was used to analyze flowing droplets one by one. A laser (488 Argon-ion Cyonics) beam was expanded (2x) and focused down with a cylindrical lens crossing orthogonally the microfluidic channel. The fluorescence signal of excited droplets was collected with a 40x objective (Olympus LUCPlanFLN, 40x/0.60), split with dichroic filter (DLP555, Semrock) and detected through bandpass filters (579/34 630/38) by Photo Multiplier Tubes (PMTs) (H957-15, Hamamatsu). Signal went through a transimpedance amplifier with 1V/uA gain and was detected by the acquisition system (National Instruments cRIO-9024, analog input module NI9223) with a 10  $\mu\text{sec}$  scan rate. The acquisition system was driven by LABView in house written software. The software detects all data-points of a droplet over a set threshold and computes in real time averaged values; it also provides trigger pulse for image capture on a camera. Liquids were pumped using neMESYS (Cetoni) syringe pumps.

*A549 quantitation.* Cultured cells were washed with PBS, trypsinized and transferred into medium (typical concentration 500,000 to 1000,000 cell/mL). Cells were spun down and resuspended in Joklik's modified EMEM (pH 7.4). If lower concentration of A549s was required, cell suspension was diluted to  $\sim 1000$  cell/mL in Joklik's modified EMEM. 100  $\mu\text{L}$  of sample solution was obtained by mixing cell suspension, SNARF-5F stock (conc. 1

---

mM) and in Joklik's modified EMEM. Fraction of obtained solution was used to verify A549 concentration in counting chamber. 1 to 2M cell/ml suspension of WBC in Joklik's modified EMEM was used to prepare samples of A549 with WBCs. Samples were emulsified at flowrate of 300  $\mu\text{L}/\text{h}$  (600  $\mu\text{L}/\text{h}$  for oil), collected in cone reservoir and incubated for 20 minutes. Droplets were reinjected from cone device directly into a readout device (50 to 100  $\mu\text{L}/\text{h}$  for droplets; 300 to 500  $\mu\text{L}/\text{h}$  for spacer oil). Detected cancerous cells were verified with images acquired for droplets with reduced pH.

*CD45 immunomagnetic depletion:* We followed manufacturer's protocol for CD45+ depletion using Miltenyi human CD45 Microbeads, MidiMACS™ Separator, MultiStand and LD Column.

*Patient protocol:* 1-2mL of whole blood from metastatic cancer patients was lysed, depleted of CD45+ fraction, CD45-Alexa488 stained and resuspended in incubation buffer, for a final volume of 50 $\mu\text{L}$  15% Optiprep.

*Patient spike protocol:* A549 cells were spiked into 1-2mL of whole blood from healthy donor and "patient protocol" was followed.

---

*References*

- 1 Green, B. J. *et al.* Beyond the Capture of Circulating Tumor Cells: Next-Generation Devices and Materials. *Angewandte Chemie International Edition* (2015).
- 2 Budd, G. T. *et al.* Circulating tumor cells versus imaging—predicting overall survival in metastatic breast cancer. *Clinical Cancer Research* **12**, 6403-6409 (2006).
- 3 Wülfing, P. *et al.* HER2-positive circulating tumor cells indicate poor clinical outcome in stage I to III breast cancer patients. *Clinical Cancer Research* **12**, 1715-1720 (2006).
- 4 Riethdorf, S. *et al.* Detection and HER2 expression of circulating tumor cells: prospective monitoring in breast cancer patients treated in the neoadjuvant GeparQuattro trial. *Clinical Cancer Research* **16**, 2634-2645 (2010).
- 5 Cohen, S. *et al.* Prognostic significance of circulating tumor cells in patients with metastatic colorectal cancer. *Annals of Oncology* **20**, 1223-1229 (2009).
- 6 Coumans, F. A., Ligthart, S. T., Uhr, J. W. & Terstappen, L. W. Challenges in the enumeration and phenotyping of CTC. *Clinical cancer research* **18**, 5711-5718 (2012).
- 7 Alix-Panabières, C. & Pantel, K. Challenges in circulating tumour cell research. *Nature Reviews Cancer* **14**, 623-631 (2014).
- 8 Willipinski-Stapelfeldt, B. *et al.* Changes in cytoskeletal protein composition indicative of an epithelial-mesenchymal transition in human micrometastatic and primary breast carcinoma cells. *Clinical Cancer Research* **11**, 8006-8014 (2005).
- 9 Bednarz-Knoll, N., Alix-Panabières, C. & Pantel, K. Plasticity of disseminating cancer cells in patients with epithelial malignancies. *Cancer and Metastasis Reviews* **31**, 673-687 (2012).
- 10 Leong, A. S., Cooper, K. & Leong, F. J. W. *Manual of diagnostic antibodies for immunohistology*. (Cambridge University Press, 2003).
- 11 Desitter, I. *et al.* A new device for rapid isolation by size and characterization of rare circulating tumor cells. *Anticancer research* **31**, 427-441 (2011).
- 12 Mani, S. A. *et al.* The epithelial-mesenchymal transition generates cells with properties of stem cells. *Cell* **133**, 704-715 (2008).
- 13 Kalluri, R. & Weinberg, R. A. The basics of epithelial-mesenchymal transition. *The Journal of clinical investigation* **119**, 1420 (2009).

- 
- 14 Qian, W., Zhang, Y. & Chen, W. Capturing Cancer: Emerging Microfluidic Technologies for the Capture and Characterization of Circulating Tumor Cells. *Small* (2015).
  - 15 Hanahan, D. & Weinberg, R. A. Hallmarks of cancer: the next generation. *cell* **144**, 646-674 (2011).
  - 16 Warburg, O., Wind, F. & Negelein, E. The metabolism of tumors in the body. *The Journal of general physiology* **8**, 519-530 (1927).
  - 17 Cardone, R. A., Casavola, V. & Reshkin, S. J. The role of disturbed pH dynamics and the Na<sup>+</sup>/H<sup>+</sup> exchanger in metastasis. *Nature Reviews Cancer* **5**, 786-795 (2005).
  - 18 Koppenol, W. H., Bounds, P. L. & Dang, C. V. Otto Warburg's contributions to current concepts of cancer metabolism. *Nature Reviews Cancer* **11**, 325-337 (2011).
  - 19 Theberge, A. B. *et al.* Microdroplets in microfluidics: an evolving platform for discoveries in chemistry and biology. *Angewandte Chemie International Edition* **49**, 5846-5868 (2010).
  - 20 Nossal, G. J. Antibody production by single cells. *British journal of experimental pathology* **39**, 544 (1958).
  - 21 Bai, Y. *et al.* A double droplet trap system for studying mass transport across a droplet-droplet interface. *Lab on a Chip* **10**, 1281-1285 (2010).
  - 22 Mazutis, L. *et al.* Single-cell analysis and sorting using droplet-based microfluidics. *Nature protocols* **8**, 870-891 (2013).

### *Microfluidic synthesis of Peptide-functionalized microgels for in serum selective protein detection*

**Abstract.** Polymeric microparticles represent a robustly platform for detection of clinically relevant analytes in biological samples; they can be functionalized with multiple types of biologics entities, enhancing their applications as a new class of colloid materials. Microfluidics offers a versatile platform for synthesis of monodisperse and engineered microparticles. Microfluidic synthesis of novel polymeric microparticles endowed with specific peptide due to its superior specificity for target binding in complex media is presented. A peptide sequence was efficiently encapsulated into the polymeric network and protein binding occurred with high affinity ( $K_D$  0.1-0.4  $\mu$ M). Fluidic dynamics simulation was performed to optimize the production conditions to obtain monodisperse and stable functionalized microgels. The results demonstrate the easy and fast realization, in a single step, of functionalized monodisperse microgels using droplet-microfluidic technique, and how the inclusion of the peptide within polymeric network improve both the affinity and the specificity of protein capture.

This work has been submitted for publication: G.Celetti; C. Di Natale; F. Causa; P.A. Netti; “**Functionalized poly(ethylene glycol) diacrylate microgels by microfluidics: in situ peptide encapsulation for in serum selective protein detection**”.

### 3.1. Introduction

Recently, hydrogels-based technologies have been developed for a wide range of biotechnology applications including diagnostic<sup>1-3</sup>, drug delivery<sup>4,5</sup> and tissue engineering<sup>6,7</sup>. Because of their biocompatibility and high tunability hydrogels represent ideal candidates for biosensing applications. Their microstructure and interfacial properties can also be rendered responsive to various stimuli through chemical and physical cues, resulting in “smart” materials which can respond to their local environment<sup>1</sup>. In particular, hydrogels can be engineered with different biological entities such as nucleic acids or peptides for capture and detection of proteins, DNA, mRNA and microRNA<sup>8</sup>. Hydrogels are typically prepared and processed as bulk materials such as monolithic structures or supported films. However, emerging applications for delivery and transport purposes in microscopic environments require miniaturization and tailoring of hydrogel architecture at increasingly small length scales. This requirement has prompted development of new methods for synthesis of hydrogel microparticles, as known as “microgels”<sup>1</sup>. Hydrogel microparticles have been suggested as diagnostic tools for the rapid multiplexed screening of biomolecules, due to their advantages in detection and quantification<sup>9-11</sup>. Compared to traditional planar arrays, particle-based arrays offer easier probe modification, more efficient mixing, and higher reproducibility<sup>12</sup>. However, appropriate methods to functionalize large microparticles have not yet been developed<sup>13</sup>. Synthesis of hydrogel microparticles in microfluidics represents one of the most promising production methods; two examples are droplet microfluidics<sup>14-16</sup> and flow lithography<sup>14</sup>. In particular, droplet microfluidics facilitates fabrication of spherical microparticles (i.e., microspheres) or microparticles with complex chemical compositions and potentially enables high throughput synthesis<sup>17</sup>. Prior reports have demonstrated the ability of microfluidic-based platforms to synthesize, functionalize and encode microparticles with multiple bioactive agents<sup>14,18,19</sup>, overcoming the conventional emulsion polymerization methods<sup>20</sup>.

Due to its biocompatibility and low-biofouling properties poly(ethylene glycol) (PEG) has been widely used for hydrogels particles-based assays. Various approaches have explored PEG’s utility as biosensor platform including direct physical entrapment<sup>21</sup> or covalently linking the biomolecules to the polymer network<sup>22</sup>.

Most of validated detection strategies use monoclonal antibodies as target recognition moieties, but the use of these large macromolecules has several limitations, including poor stability and high production costs<sup>23,24</sup>. In contrast, small molecules like peptides can be prepared synthetically and they mimic the antibody binding site by using only a small cluster of residues, even though with lower affinity and specificity toward biomolecule target<sup>25</sup>. Hydrogel networks endowed with bioactive peptides have been already reported for applications such as tissue engineering, where short peptide sequences were demonstrated to elicit specific cell functions or change the materials network upon specific cell responses<sup>26</sup>. However, the capability of hydrogel microparticles, functionalized with small molecules in a single step, to increase the affinity and the specificity of a protein capture has not yet been explored.

Here, droplet microfluidics is used for one step synthesis of monodisperse and stable micrometer poly(ethylene glycol) diacrylate (PEGDA) hydrogels. A reactive and labeled peptide sequence was incorporated in the microgels to create a functional microparticles for selective protein detection in complex fluid (**Figure 3.1**), eliminating the need for costly and time-consuming labeling steps. Computational fluidic dynamics simulation (CFD) was used to optimize the design of the device investigating the parameters that influence droplet formation. Protein detection in buffer and in complex biological medium was demonstrated by confocal technique. This approach promises to be useful for producing a novel, efficient and sensitive polymeric microparticles to detect bio-molecular targets with higher affinity in complex medium.

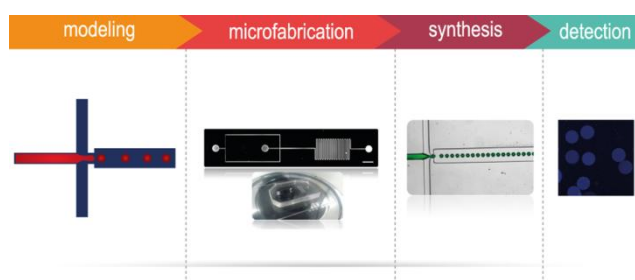


**Figure 3.1:** Schematic representation of Strep-tag II-microparticles synthesis able to detect Streptavidin protein in human serum. Such approach includes: phase modelling; microfluidic fabrication and validation; microgel synthesis; and assay validation for selective protein detection.

## 3.2. Results and discussion

### 3.2.1. Microfluidic design

Microfluidic design (**Figure 3.2**), was optimized to obtain monodisperse and stable functional microgels in order to create a tool-system for biosensing.

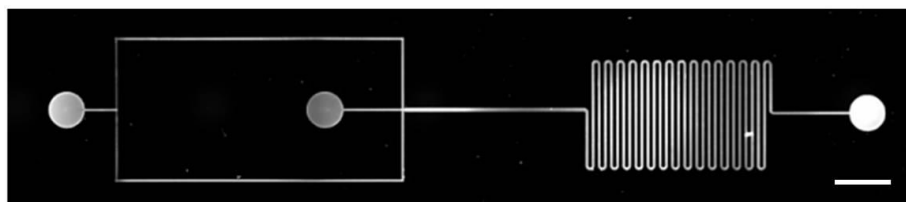


**Figure 3.2:** Schematic representation of FFD for Strep-tag II-microparticles synthesis.

Droplet formation process is affected by several physical parameters such as flow rates, viscosity of the fluids, dimensions of the geometry, Capillary number ( $Ca$ ) and surface tension<sup>15</sup>; therefore, the design of optimal microfluidic device for the production of monodisperse and stable emulsion relies on controlling such parameters.

In the first set of simulations the influence of geometry and  $Ca$  on droplet production was investigated. Firstly, the dimensions of the device junction were changed; in particular, different widths and lengths were modeled. Based on the simulation results,  $50 \times 35 \times 50$  (width  $\times$  depth  $\times$  length) were the chosen dimensions of the junction in the region of droplet formation.

Droplet formation is driven by the competition between the viscous stress and the surface tension of two immiscible fluids, this occurs at a critical Capillary number<sup>27</sup>. For this, the influence of  $Ca$  on emulsion stability was investigated, maintaining geometry device constant.  $Ca$  can be modified by varying the

flow rate of the continuous phase ( $Q_{oil}$ ). Simulation results shows three different flow patterns after the junction: elongation flow pattern, stable emulsions and unstable emulsions (**Figure 3.3 A, B, C**). It is difficult generate stable emulsion at high flow

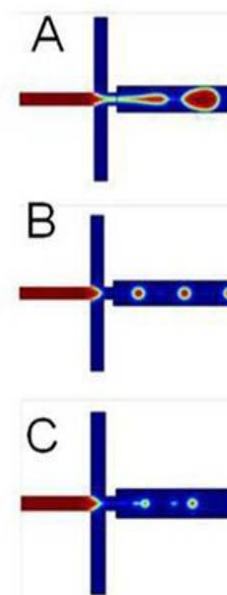


**Figure 3.3:** Three distinct regions were observed: a) elongation flow of thread, b) stable droplets, (c) unstable droplet formation

---

rates of prepolymer solution ( $Q_p > 5 \mu\text{l}/\text{min}$ , in this case); in fact, W/O emulsion could not separate uniformly from the junction due to the unstable hydrodynamic pressure of PEGDA prepolymer phase. When the value of  $Ca$  is in a limited range  $0.005 \sim 0.055$ , the prepolymer phase breaks into a stable emulsion (regime of stable emulsions **Figure 3.3B**). Choi et al. also investigated flow patterns to obtain stable polymeric droplets<sup>28</sup>.

Precise control of particle size and monodispersity is critical for many applications of microgels; microfluidic platform provides control over a wide range of sizes. For this reason, in the second set of simulations the influence of  $Q_{oil}$  on the droplet size was investigated, while  $Q_p$  was kept constant. Once the dimensions of the device have been fixed, microgels with a wide range of sizes, ranging from  $10$  to  $90 \mu\text{m}$ , were produced. Droplets diameters were calculated during simulation analysis. In particular, a droplet size was determined by the flow rates of the two phases and the ratio between these flow rates, as proposed by Collins et al. Maintaining the ratio of the two flow rates constant, droplets size decreases as  $Q_{oil}$  increases.

In order to stabilize droplets against uncontrolled coalescence, the use of surfactant is necessary. These amphiphilic molecules are commonly used to stabilize the droplet interface and to prevent coalescence of droplets<sup>16</sup>. The interfacial tension is strongly dependent on the surfactant's local surface coverage, but, in turn, it affects significantly droplet size and stability during emulsification<sup>27</sup>. The interfacial tension between the two phases is influenced by the viscosities of the fluids. **Figure 3.4** show the correlation between the polymer's concentration in the disperse phase and its viscosity. Increasing the amount of the polymer, the viscosity of the disperse phase increases resulting in a loss of droplets' stability.

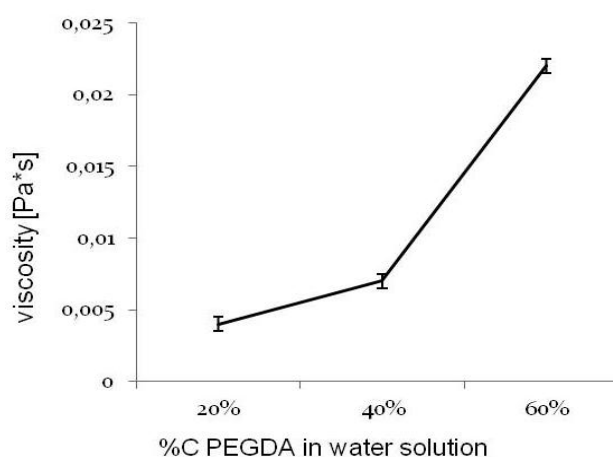


**Figure 3.4:** measures of PEGDA viscosity solution at 20%, 40%, 60% wt. through 50 mm flat-plate geometry by rheometer. The viscosity increase when the concentration of PEGDA in water solution (disperse phase) increase.

If the prepolymer concentration is lower than 20 wt %, its solution can be used to form droplets, but required UV curing is long and these droplets deform and damage easily<sup>8</sup>. In contrast, a solution with PEGDA concentration higher than 60 wt % can be cured by UV light in less time; but it is difficult to control the stability of the droplets because of their high viscosity<sup>29</sup>. A dispersed phase at 20 wt.% of PEGDA was chosen, setting the length of the circuit in the device at 10 cm for droplets polymerization directly in flow using the UV lamp of the microscope.

### 3.2.2. PEGDA peptide-microgels synthesis and characterization

Here microfluidic synthesis of biodegradable PEGDA peptide-microgels for diagnostic applications is reported. The encapsulated peptide (Strep-tagII) contains sequence of eight amino acid ( $H_2N$ -WSHPQFEK-COOH) selected from a random peptide library as an artificial ligand for streptavidin protein<sup>30</sup>. It is usually used for efficient protein purification in a single step and it is also important in the study of metallo-proteins<sup>31</sup>. The peptide was labeled with fluorophor for verification of its encapsulation. Microgels formation is shown in **Figure 3.5** and described in Experimental Section. Briefly, the pre-polymer solution containing Strep-tagII-FITC peptide was injected through the central channel of the microfluidic device, as disperse phase, and oil solution with surfactant through its two

opposite side channels, as continuous phase. Disperse phase was sheared into monodisperse droplets by continuous phase.

Microfluidic set up allows robust and rapid synthesis of functional and uniform polymeric microparticles in a single step, overcoming the limits of the conventional suspension polymerization methods. Strep-tagII-microgels are monodisperse in size with a coefficient of polydispersity (PDI) < 0.003 and the homogeneity of the peptide inside the microgels ( $\approx 1.31$  pg of peptide in each microgel) was confirmed by confocal image (**Figure 3.6**). Uniform particle size and homogeneous peptide labeling make this approach promising for selective protein detection.

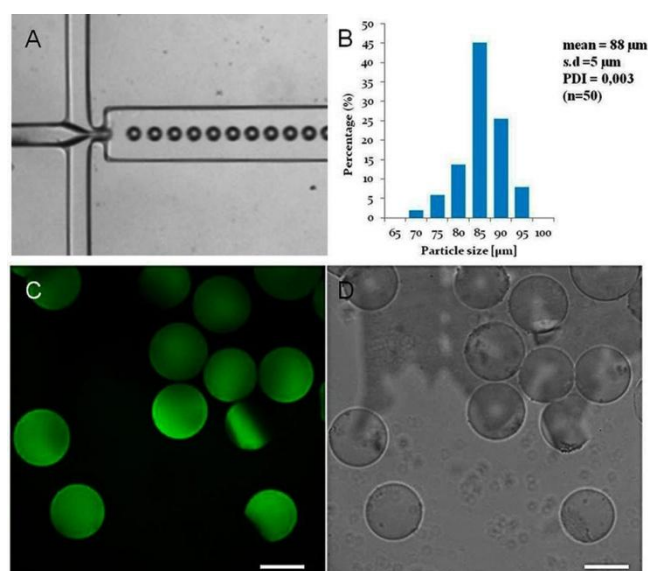


**Figure 3.5:** PEGDA-peptide microgel (20% PEGDA, 0.1% Darcour, 0.5 mg/mL peptide). (A) Strep-tagII microgels synthesis by microfluidic device. (B) Size distribution of PEGDA-peptide microgels. (C) Fluorescent image of Strep-tagII-FITC encapsulation. (D) Phase contrast image of microgels. Scale bars are 100 μm.

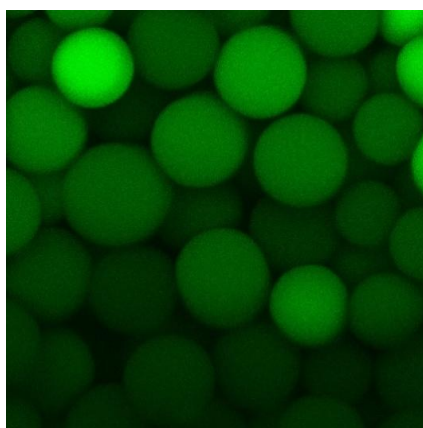


**Figure 3.6:** image 3D of PEGDA Strep-Tag-II, confirm the homogeneity of the peptide inside microgels.

Despite the addition of biologic entities may lead to a slight increase in the deviation of diameter, the resulting microgels remained largely uniform, thereby demonstrating the ability of our approach to encapsulate biomolecules in polymeric microparticles.

PEGDA has been chosen for its advantages over other polymers and its specific proprieties, such as good biocompatibility, non-toxicity, low immunogenicity in vivo, and resistance to protein adsorption. Moreover, polyethylene glycol (PEG) hydrogels are widely used in biomedical fields such as drug delivery and tissue engineering<sup>32</sup>

Finally, to verify the secondary structure of the peptide in solution and inside microgels, circular dichroism (CD) was performed. CD spectra of peptide registered in aqueous buffer solution (**Figure 3.7A**) revealed a random coil content due to the absence of Cotton bands at 205, 222 nm that are typical of helix conformations. As showed in figure 3.7A the addition of different TFE concentrations results in an increase of helical content, in particular at 60% of TFE peptide spectrum shows a presence of little Cotton bands at 205 and 222 nm. The same experiments were carried out for peptide incorporated into the microgels. CD data confirmed that Strep-tagII peptide retains its structure (random-coil as it expect for small peptides) after its encapsulation, as previously reported for other peptides<sup>33</sup>. **Figure 3.7B** shows CD spectrum of Step-tagII peptide and Strep-TagII microgels. In order to analyze the structural behavior of the peptide encapsulated into the microgels, CD spectrum at 60% of TFE was recorded. In contrast of peptide spectrum at 60% of TFE, peptide encapsulated didn't change its conformation even with high TFE content, showing only a slight band at 220nm. **Figure 3.7C** and **D** show CD data of Strep-

tagII-microgels recorded at 0 and 60% of TFE and peptide spectrum in solution and incorporated inside microgels at the same TFE concentration.

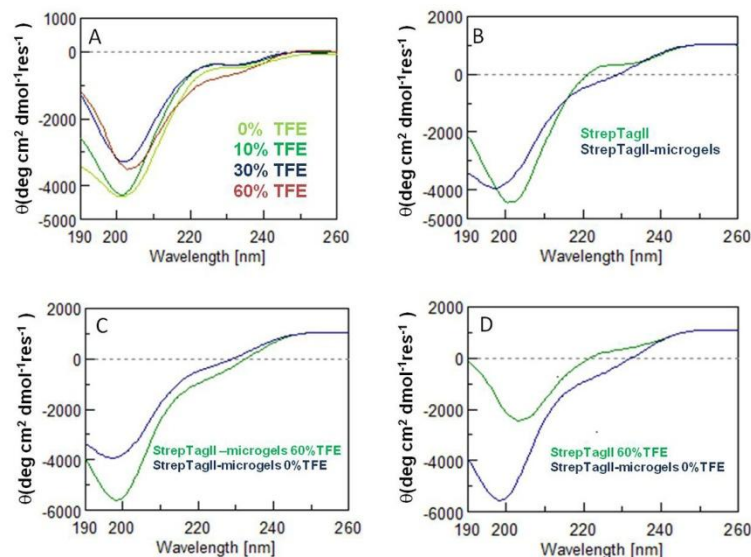


**Figure 3.7:** CD analysis of Strep-tagII peptide and Strep-tagII peptide-microgels, in phosphate buffer 10 mM pH 7. Overlay of Strep-tagII peptide CD spectra recorded (A) with increasing amounts of TFE (from 0 to 60%), Overlay of StreptagII-peptide and StreptagII-microgels CD spectra in buffer solution (B), Overlay of StrepTagII microgels CD spectra recorded (C) with 0% and 60% of TFE and Overlay of StrepTagII peptide and microgels recorded (D) with 60% of TFE.

Importantly, our strategies is relatively simple and robust, and encapsulated molecules retain their structure during microgels processing. Moreover, we demonstrate that CFS allow a robust control over microgels synthesis, avoiding fabrications of many different microfluidic devices.

### 3.2.3. Protein-binding analysis in PBS and human serum

One motivation for using peptides in polymeric networks for protein detection is to employ them to have a selective protein detection in complex mixtures<sup>34</sup>. Protein-binding peptide is described in more details in Experimental Section. Different concentrations of Streptavidin protein (labeled with Atto-425), ranging from 0.16  $\mu\text{M}$  to 1.6  $\mu\text{M}$ , were used in the experiment. **Figure 3.8B** shows Streptavidin-Atto-425 fluorescence on Strep-tagII-microgels in PBS. The selective binding of protein was demonstrated using the same

protocol for Control-microgels labeled with rhodamine B (**Figure 3.8E**). Atto-425 fluorescence signal occurred only on Strep-tagII-microgels and its intensity increased with increasing protein concentration (**Figure 3.8L**) in sample, giving a reasonably specific binding signal.

Most important is to test binding in complex mixtures where other interfering proteins are in abundance. We evaluated the accuracy of our system directly in biological environment. Fluorescence image (**Figure 3.8H**) confirms protein-binding peptide and the accuracy of the microgel-based assay also in complex matrix.

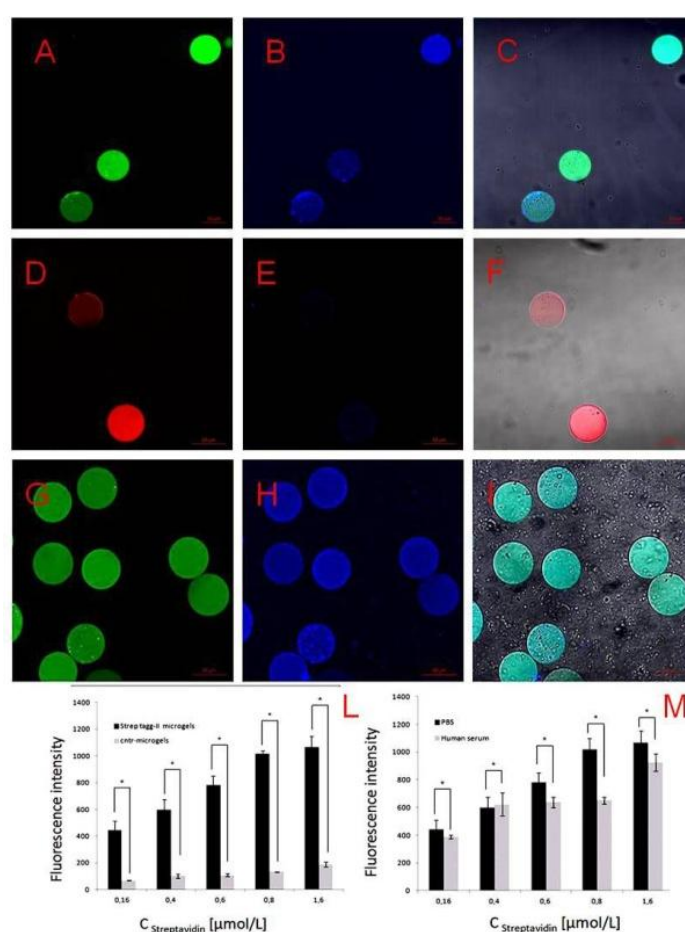


**Figure 3.8:** Fluorescence detection of specific and unspecific binding both in PBS and in human serum. Single component detection: (A) strep-tagII-microgels (green) and (B) Streptavidin binding microgels (blue); (C) Overlay image. The single component images demonstrate that there is no occurrence of overlapping signals. (D) PEGDA microgels labeled with Rhodamine B (red) as a control of unspecific signal; (E) fluorescence image of streptavidin on control microgels; (F) overlay channel; (G) Strep-tagII-microgels (green) and (H) Streptavidin binding microgels (blue) in human serum; (I) Overlay image for specific protein-binding peptide in human serum; (L) Bioassay

system efficiency of microgels-bounding; (M) Performance of bioassay system for protein detection in PBS and in human serum. The binding event is detected by measuring the fluorescence intensity of Atto-425 conjugated Streptavidin directly on 50 microgel particles. Statistical difference between Strep tag II-microgels and control microgels  $*p < 0.05$  (mean $\pm$ SD n=2) in PBS and  $*p > 0.05$  (mean $\pm$ SD n=2) in human serum.

It is evident that Streptavidin-Atto-425 recognition is specific and dose-response (**Figure 3.9A**), with an estimated  $K_D$  of  $0.40 \pm 0.11 \mu\text{M}$ , which demonstrate a good affinity toward Streptavidin protein. As reported the maximum constant affinity between such peptide and protein is about  $70 \mu\text{M}$ <sup>35,36</sup>, therefore microgel is able to improve the sensitivity and specificity of protein detection. We observed that there was no obvious change of fluorescent intensity when the concentration of Streptavidin-Atto-425 was higher than  $1.6 \mu\text{M}$ . Thus the saturation point of Streptavidin-Atto-425 was higher than  $1.6 \mu\text{M}$  in PBS.

Moreover **Figure 3.9B** shows that the fluorescence intensity of the Streptavidin-Atto-425 is dose-responsive and specific in serum as well, with a  $K_D$  of  $0.12 \pm 0.047 \mu\text{M}$ <sup>37</sup>. Such performance is ascribable to the capability of the polymeric network to offer antifouling properties, thus improving the specificity of the capture.

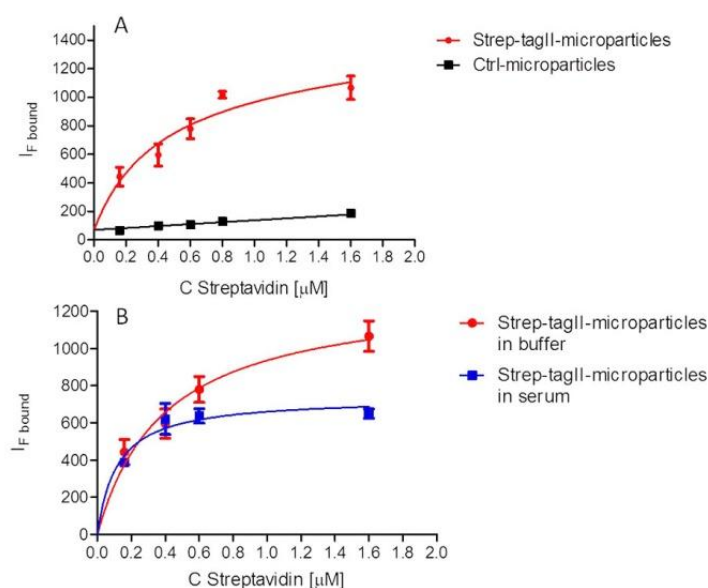


**Figure 3.9:** Strep-tagII-microgels-protein binding confocal results. (A) the Streptavidin-ATTO-425 recognition (red curve) is specific, unlike Control-microgels (black curve) (mean $\pm$ SD n=2). (B) Comparison of confocal binding by non linear fitting in buffer (red curve) and in serum (blue curve).

We synthesized functional microgels for selective protein detection both in PBS and in complex fluid, using droplet-microfluidics. This method is relative simple, rapid and support the use of microfluidic device as a manufacturing platform for biosensing.

We believe that the reported system can be broadly applicable for rapid synthesis of microgels for different application like food contaminants detection, using different small molecules.

### ***3.3. Conclusions***

Here we report droplet-microfluidics for the easy and rapid synthesis of biodegradable PEGDA peptide-microgels for selective biomolecules capture in complex medium, unlike conventional techniques. Based on numerical simulations, we fabricate microfluidic device to produce stable and monodisperse microgels. Uniform distribution of the specific peptide within the microgel was achieved and the efficiency of peptide-to-protein binding both in PBS and human serum was confirmed. These functional microparticles allows the enhancement of binding affinity and the specificity in complex media.

Our system is simple and flexible towards the detection of different molecules, does not require preliminary treatments of the sample and allows for the specific detection in complex fluid because of its antifouling properties. The control of physical and chemical properties of microgels through droplet microfluidics and the flexibility to encapsulate different molecules make our method useful for any direct bio-detection in complex fluids.

### ***Acknowledgments***

Concetta Di Natale is acknowledged for design peptide synthesis protocol and CD analysis. Vincenzo Calcagno and Francesco del Giudice are gratefully acknowledged for fruitful discussion. Armando Cosentino is acknowledged for laser 2D training.

### ***3.4. Experimental Section***

*General Materials and Method.* Poly(ethylene glycol) diacrylate (PEGDA, 700 MW), the non polar solvent light mineral oil and the nonionic detergent sorbitan monooleate (Span 80) were purchased from Sigma Aldrich. Crosslinking reagent Darocur 1173 was purchased from Ciba. Reagents for peptide synthesis (Fmoc-protected amino acids, resins,

activation, and deprotection reagents) were purchased from Iris Biotech GmbH (Waldershofer Str. 49-51 95615 Marktredwitz, Deutschland) and InBios (Naples, Italy). Solvents for peptide synthesis and HPLC analyses and Streptavidin ATTO-425 were purchased from Sigma-Aldrich; reversed phase columns for peptide analysis and the LC-MS system were supplied respectively from Agilent Technologies and Waters (Milan, Italy). Pooled human serum from healthy donors was supplied by Lonza (Life Technology Ltd, Paisley, UK). All chemicals were used as received.

*Microfluidic device fabrication.* Microfluidic device consists of two inlets for the continuous and disperse phase, a narrow orifice in which the main channel and the two opposite channels converge, and a serpentine in which droplets were polymerized. The dimensions of the microchannel dimensions in the region of droplet formation is  $50 \times 35 \times 50$  (width  $\times$  depth  $\times$  length); the serpentine is 10 cm long. The microfluidic device was fabricated by combining the conventional photolithographic and soft-lithographic techniques. Briefly, negative photoresist (Mr-DWL 40 photoresist, Microresist technology) was spun onto a silicon wafer at 2000 rpm for 30 s to make a 35  $\mu\text{m}$  thick layer of photoresist. Then, the photoresist was baked and subsequently exposed using DWL 66 Fs LASER technology system (Heidelberg instruments). After the exposed sample had been post-baked and developed, the microfluidic flow focusing device master was prepared. The surface of the device mold was treated with tridecafluoro-1,1,2,2-tetrahydrooctyl-1-trichlorosilane to facilitate the peeling off of the polydimethyl-siloxane (PDMS, Sylgard 184, Dow Corning) replica. PDMS (10:1 polymer to curing agent) was poured on the patterned silicon wafer containing negative-channels. The PDMS-based microfluidic device was peeled off from the wafer and bonded on a glass slide with oxygen plasma treatment.

*Computational Fluid Dynamic simulation.* To optimize the design of the device, computational fluid dynamics simulations were performed using COMSOL Multiphysics 4.2b software. During the simulation, all geometries were created two-dimensional based on the dimensions of the designed microfluidic device. A two-dimensional model was chosen to reduce complexity and computation time. The momentum and mass balances were modeled by Navier-Stokes equations and the level set method (LSM) was used to model the two phases. The principle on which LSM is based is the assignment of a so-called level set function  $\Phi(x, t)$  to the space occupied by an interface, where  $x$  denotes the

co-ordinates of a point within that space at a time  $t$ . The function is initialized at time  $t_0$ , and then a numerical scheme is used to approximate the value of  $\Phi(x, t)$  over small time increments, thus enabling the propagation of the interface to be tracked in time. The interface is represented by the zero contour of the level set function  $\Phi$ .  $\Phi > 0$  on one side of the interface and  $\Phi < 0$  on the other. The level set function is chosen such that the position of the water–oil interface is described by the 0.5 contour of the level set function  $\Phi$  and for  $\Phi > 0.5$  the break off occurs and the droplet is formed. Channel geometries were meshed using the free meshing tool and the channel walls were specified as wetted walls with a constant contact angle, measured experimentally using the instrument Contact Angle CAM 200. The interfacial tension between the continuous phase and the prepolymer solution was changed to investigate the influence of the surface tension ( $\gamma$ ) on the droplet sizes.  $\gamma$  was measured by pendant drop CAM 200. The viscosity of the two fluids was measured with 50 mm flat-plate geometry by rheometer.

*Synthesis of Strep-TagII peptide.* Strep-tagII-peptide ((WSHPQFEKD(OAll))) synthesis was performed on a fully automated multichannel peptide synthesizer Biotage® Syro Wave™. Preparative RP-HPLC was carried out on a Waters 2535 Quaternary Gradient Module, equipped with a 2489 UV/Visible detector and with an X-Bridge™ BEH300 preparative 10× 100 mm C18, 5 $\mu$ m column. LC–MS analyses were carried out on an Agilent 6530 Accurate-Mass Q-TOF LC/MS spectrometer. Zorbax RRHD Eclipse Plus C18 2.1 x 50 mm, 1.8  $\mu$ m columns were used for the analyses. The Strep-tagII-peptide was synthesized in the acetylated/amidate version, employing the solid phase method on a 50  $\mu$ mol scale following standard Fmoc strategies. Rink-amide resin (substitution 0.45 mmol/g) was used as solid support. Activation of amino acids was achieved using HBTU/HOBt/DIPEA (1:1:2). All couplings were performed for 15 min and deprotections for 10 min. To monitor peptide entrapment, Lysine side chain amine fluorescein labeling was achieved by on-resin treatment with fluorescein isothiocyanate (FITC) after removing methyltrityl (Mtt) protecting group using 1% TFA in DCM for 30 min. Peptide was then removed from the resin, by treatment with a TFA/TIS/H<sub>2</sub>O (95:2.5:2.5, v/v/v) mixture for 90 min at room temperature; then, crude peptide was precipitated in cold ether, dissolved in a water/acetonitrile (1:1, v/v) mixture, and lyophilized. Product was purified by RP-HPLC applying a linear gradient of 0.1% TFA CH<sub>3</sub>CN in 0.1% TFA water from 5% to 70% over 30 min using an X-Bridge™ BEH300 preparative 10× 100 mm C18, 5 $\mu$ m

column at a flow rate of 10 mL/min. Peptide purity (95%) and identity (1488 amu) was confirmed by LC–MS (data not shown). Purified peptide was lyophilized and stored at  $-20\text{ }^{\circ}\text{C}$  until use.

*Synthesis of functional microgels.* Microgels were synthesized using light mineral oil containing nonionic surfactant Span 80 (3 wt%) as a continuous phase and poly(ethylene glycol)diacrylate (PEGDA) (20 wt%) with photoinitiator (0.1 wt%) and Strep-tagII-FITC (0.5 mg/mL) as a disperse phase. Droplets were formed injecting prepolymer solution, disperse phase, through the central channel and oil solution, continuous phase, through two opposite side channels. The uniform PEGDA-peptide droplets were crosslinked in flow to form monodisperse microgels. To photopolymerize droplets DAPI microscopy filter (9.8 mW,  $\lambda=360\text{ nm}$ ) was used, focusing the UV light on the serpentine and regulating the diaphragm aperture of the microscope, for 15s. After photopolymerization, microgels were collected in an eppendorf and washed three times with a solution of ethanol (35 v/v%) and acetone (10 v/v%) to remove the oil. After washing, microgels containing Strep-tagII-FITC were analyzed by confocal microscopy. Polyethylene tubes were connected to the inlets and outlets and the solutions were injected using high-precision syringe pumps (neMesys-low pressure) to ensure a reproducible, stable flow. This system was mounted on an inverted microscope (IX 71 Olympus) and the droplets formation was visualized using a 4 $\times$  objective and recorded with a CCD camera Imperx IGV-B0620M.

*Protocol of peptide encapsulation and protein-binding analysis.* Peptide was encapsulated adding Strep-tagII-FITC (0.5 mg/mL) to the disperse phase prior to microgel synthesis. Fluorescent microgels without peptide, used as negative control, were obtained dissolved 0.1 mg of Rhodamine B in 10 mL of water solution. Binding experiments were performed incubating Strep-tagII-microgels and microgels without peptide (Control-microgels) with Streptavidin-Atto-425 (peptide/protein ratio 5/1) in PBS (pH 7.4) and human serum from healthy donors (final volume 200 mL) at room temperature for 2 h. After incubation Strep-tagII-microgels and Control-microgels were centrifuged for 5 min at 10000 rpm and the supernatant was measured by fluorescence spectroscopy ( $\lambda_{\text{exc}}\ 436 - \lambda_{\text{em}}\ 484$ ) using a Perkin Elmer 2300 Enspire Plate Reader.

To demonstrate the ability of our system to detect specific protein, 100  $\mu\text{L}$  of Strep-tagII-microgels were suspended in 1 mL of PBS and different concentrations of Streptavidin protein, ranging from 0.16  $\mu\text{M}$  to 1.6  $\mu\text{M}$ , were added and these solutions were incubated

---

for 2 h. After the incubation, microgels were washed three times and their fluorescence was analyzed. The same protocol was used for microgels without peptide, as a negative control, and for *Strep-TagII*-microgels in serum analysis as well.

*Confocal Microscopy.* Microgels images, before binding, were collected with Leica confocal microscope SP5 (Leica Microsystems), provided with an HCX IRAPO L 25.0×/0.95 WATER objective and an Argon laser (488 nm as selected wavelength) as excitation sources for FITC-peptide. Detection occurred at the 500-530 nm band. Images have been acquired with a resolution of 1024 × 1024 pixels, zoom 1, 2.33 A.U. pinhole. All our experiments were performed at room temperature.

Fluorescence analysis of protein-binding was performed by Zeiss LSM700 confocal microscope, using 20× dry objective. Two-channel fluorescence images were acquired, simultaneously, using multitrack mode. 480 nm and a 405 nm DAPI solid state lasers as excitation sources were used for peptide-FITC and Streptavidin-Atto-425-protein 435, respectively. Fluorescence was detected at 500-530 nm and 410-450 nm bands, respectively.

*Circular Dichroism analysis.* CD spectra were recorded using a JascoJ-1500 spectropolarimeter in a 1.0 cm quartz cell at room temperature. The spectra were recorded from 300 to 190 nm, with a band width of 1 nm, a time constant of 16 s, and a scan rate of 10 nm/min. Blank samples were subtracted from all recorded spectra.

*Statistical analysis.* The results of confocal experiments were analyzed by software GraphPad Prism version 5.04 and experimental data were expressed as mean ± standard deviation. One-tailed analysis of variance with an Unpaired t-Test was performed to compare all experimental groups and to determine statistical significance of  $p < 0.05$ . The evaluation of  $K_D$  was calculated by a non-linear fitting approach using GraphPad Prism version 5.04 software.

---

### References

- 1 Helgeson, M. E., Chapin, S. C. & Doyle, P. S. Hydrogel microparticles from lithographic processes: Novel materials for fundamental and applied colloid science. *Current opinion in colloid & interface science* **16**, 106-117 (2011).
- 2 Langer, R. & Tirrell, D. A. Designing materials for biology and medicine. *Nature* **428**, 487-492 (2004).
- 3 Rubina, A. Y., Kolchinsky, A., Makarov, A. A. & Zasedatelev, A. S. Why 3-D? Gel-based microarrays in proteomics. *Proteomics* **8**, 817-831 (2008).
- 4 Peppas, N. A., Hilt, J. Z., Khademhosseini, A. & Langer, R. Hydrogels in biology and medicine: from molecular principles to bionanotechnology. *ADVANCED MATERIALS-DEERFIELD BEACH THEN WEINHEIM-* **18**, 1345 (2006).
- 5 Peppas, N. A., Keys, K. B., Torres-Lugo, M. & Lowman, A. M. Poly (ethylene glycol)-containing hydrogels in drug delivery. *Journal of controlled release* **62**, 81-87 (1999).
- 6 Lee, K. Y. & Mooney, D. J. Hydrogels for tissue engineering. *Chemical reviews* **101**, 1869-1880 (2001).
- 7 Nguyen, K. T. & West, J. L. Photopolymerizable hydrogels for tissue engineering applications. *Biomaterials* **23**, 4307-4314 (2002).
- 8 Le Goff, G. C., Srinivas, R. L., Hill, W. A. & Doyle, P. S. Hydrogel microparticles for biosensing. *European Polymer Journal* (2015).
- 9 Birtwell, S. & Morgan, H. Microparticle encoding technologies for high-throughput multiplexed suspension assays. *Integrative Biology* **1**, 345-362 (2009).
- 10 Wilson, R., Cossins, A. R. & Spiller, D. G. Encoded Microcarriers For High-Throughput Multiplexed Detection. *Angewandte Chemie International Edition* **45**, 6104-6117 (2006).
- 11 Pregibon, D. C., Toner, M. & Doyle, P. S. Multifunctional encoded particles for high-throughput biomolecule analysis. *Science* **315**, 1393-1396 (2007).
- 12 Bong, K. W., Chapin, S. C. & Doyle, P. S. Magnetic barcoded hydrogel microparticles for multiplexed detection. *Langmuir* **26**, 8008-8014 (2010).
- 13 Kim, J. H. *et al.* Droplet microfluidics for producing functional microparticles. *Langmuir* **30**, 1473-1488 (2013).

- 
- 14 Duncanson, W. J. *et al.* Microfluidic synthesis of advanced microparticles for encapsulation and controlled release. *Lab on a Chip* **12**, 2135-2145 (2012).
- 15 Dendukuri, D. & Doyle, P. S. The synthesis and assembly of polymeric microparticles using microfluidics. *Advanced Materials* **21**, 4071-4086 (2009).
- 16 Baret, J.-C. Surfactants in droplet-based microfluidics. *Lab on a Chip* **12**, 422-433 (2012).
- 17 Nisisako, T. & Torii, T. Microfluidic large-scale integration on a chip for mass production of monodisperse droplets and particles. *Lab on a Chip* **8**, 287-293 (2008).
- 18 Xu, Q. *et al.* Preparation of monodisperse biodegradable polymer microparticles using a microfluidic flow-focusing device for controlled drug delivery. *Small* **5**, 1575-1581 (2009).
- 19 Kesselman, L. R., Shinwary, S., Selvaganapathy, P. R. & Hoare, T. Synthesis of Monodisperse, Covalently Cross-Linked, Degradable “Smart” Microgels Using Microfluidics. *Small* **8**, 1092-1098 (2012).
- 20 Causa, F., Aliberti, A., Cusano, A. M., Battista, E. & Netti, P. A. Supramolecular spectrally encoded microgels with double strand probes for absolute and direct miRNA fluorescence detection at high sensitivity. *Journal of the American Chemical Society* **137**, 1758-1761 (2015).
- 21 Torres-Lugo, M. & Peppas, N. A. Preparation and characterization of P (MAA-g-EG) nanospheres for protein delivery applications. *Journal of Nanoparticle Research* **4**, 73-81 (2002).
- 22 Zisch, A. H. *et al.* Cell-demanded release of VEGF from synthetic, biointeractive cell ingrowth matrices for vascularized tissue growth. *The FASEB journal* **17**, 2260-2262 (2003).
- 23 Chirinos-Rojas, C. L., Steward, M. W. & Partidos, C. D. A peptidomimetic antagonist of TNF- $\alpha$ -mediated cytotoxicity identified from a phage-displayed random peptide library. *The Journal of Immunology* **161**, 5621-5626 (1998).
- 24 Cusano, A. M. *et al.* Integration of binding peptide selection and multifunctional particles as tool-box for capture of soluble proteins in serum. *Journal of The Royal Society Interface* **11**, 20140718 (2014).
- 25 Banner, D. W. *et al.* Crystal structure of the soluble human 55 kd TNF receptor-human TNF $\beta$  complex: implications for TNF receptor activation. *Cell* **73**, 431-445 (1993).

- 
- 26 Jing, J., Fournier, A., Szarpak-Jankowska, A., Block, M. R. & Auzély-Velty, R. Type, Density, and Presentation of Grafted Adhesion Peptides on Polysaccharide-Based Hydrogels Control Preosteoblast Behavior and Differentiation. *Biomacromolecules* **16**, 715-722 (2015).
- 27 Baroud, C. N., Gallaire, F. & Dangla, R. Dynamics of microfluidic droplets. *Lab on a Chip* **10**, 2032-2045 (2010).
- 28 Choi, C.-H., Jung, J.-H., Hwang, T.-S. & Lee, C.-S. In situ microfluidic synthesis of monodisperse PEG microspheres. *Macromolecular Research* **17**, 163-167 (2009).
- 29 Dang, T.-D., Kim, Y. H., Kim, H. G. & Kim, G. M. Preparation of monodisperse PEG hydrogel microparticles using a microfluidic flow-focusing device. *Journal of Industrial and Engineering Chemistry* **18**, 1308-1313 (2012).
- 30 Schmidt, T. G. & Skerra, A. The random peptide library-assisted engineering of a C-terminal affinity peptide, useful for the detection and purification of a functional Ig Fv fragment. *Protein Engineering* **6**, 109-122 (1993).
- 31 Korndörfer, I. P. & Skerra, A. Improved affinity of engineered streptavidin for the Strep-tag II peptide is due to a fixed open conformation of the lid-like loop at the binding site. *Protein science* **11**, 883-893 (2002).
- 32 Chung, B. G., Lee, K.-H., Khademhosseini, A. & Lee, S.-H. Microfluidic fabrication of microengineered hydrogels and their application in tissue engineering. *Lab on a Chip* **12**, 45-59 (2012).
- 33 Black, K. A. *et al.* Protein encapsulation via polypeptide complex coacervation. *ACS Macro Letters* **3**, 1088-1091 (2014).
- 34 Zhang, Z., Zhu, W. & Kodadek, T. Selection and application of peptide-binding peptides. *Nature biotechnology* **18**, 71-74 (2000).
- 35 Skerra, A. & Schmidt, T. G. Applications of a peptide ligand for streptavidin: the Strep-tag. *Biomolecular engineering* **16**, 79-86 (1999).
- 36 Freitag, S. *et al.* X-ray crystallographic studies of streptavidin mutants binding to biotin. *Biomolecular engineering* **16**, 13-19 (1999).
- 37 EL-Sharif, H. F., Hawkins, D. M., Stevenson, D. & Reddy, S. M. Determination of protein binding affinities within hydrogel-based molecularly imprinted polymers (HydroMIPs). *Physical Chemistry Chemical Physics* **16**, 15483-15489 (2014).

### *Label-free method for aflatoxin detection: microfluidic microgels functionalized with two novel peptides*

**Abstract.** A novel method using droplet microfluidics for aflatoxin M<sub>1</sub> (AFM<sub>1</sub>) detection is presented. AFM<sub>1</sub> is the most toxic, carcinogenic, teratogenic and mutagenic class of aflatoxins (AFs) and is present in a wide range of food and feed commodities, such as milk and dairy products. In the last ten to twenty years the presence of AFM<sub>1</sub> in such products has been an important issue world, especially for developing countries. In this work poly(ethylene glycol) dyacrilate (PEGDA) functionalized microparticles, as a novel tool for sensitive and label-free detection of aflatoxin M<sub>1</sub> (AFM<sub>1</sub>), were synthesized. PEGDA microparticles were produced and functionalized through droplet microfluidic device. Two novel peptides, synthesized for specific aflatoxin detection, were encapsulated into the microgels directly in flow. AFM<sub>1</sub> detection was achieved measuring its innate fluorescence. The fluorescent signal increased with the increment of AFM<sub>1</sub> concentration in sample. The detection limit of this technique for AFM<sub>1</sub> was estimated to be 1.64 ng/Kg, with a dynamic detection range between 3.28 ng/Kg and 656 ng/Kg, which meets present legislative limits of 50 ng/Kg. Therefore, the developed systems, using microfluidics, provides a promising approach for rapid screening of food contaminates because it is simple, sensitive, specific, without the need of multiple separation steps, overcoming the limits of the traditional AFM<sub>1</sub> capture methods, which are expensive and time consuming.

## 4.1. Introduction

AFM<sub>1</sub>, a hydroxylated metabolite of aflatoxin B<sub>1</sub>, is often found in milk from animals fed with aflatoxin B<sub>1</sub>-contaminated feeds (**Figure 4.1**)<sup>1,2</sup>. AFM<sub>1</sub> can be also found in a variety of dairy products such as cheese, yogurt, and infant formula due to its resistance to heat treatment<sup>3</sup>. AFM<sub>1</sub> is the most toxic, carcinogenic, teratogenic and mutagenic class of aflatoxins<sup>4</sup>. Therefore, the contamination of foods by AFM<sub>1</sub> could pose a serious risk to public health, especially to milk consumers.

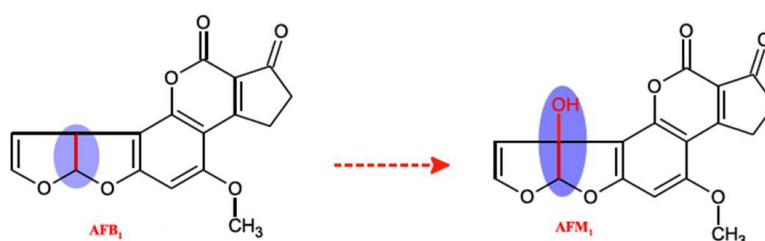


**Figure 4.1:** schematic representation of AFM<sub>1</sub>

The EU limits the total AF levels to no more than 0.05 µg/Kg in milk (the United States Food and Drug Administration established action levels for AF concentration of 0.5 µg/Kg, however the Codex Alimentarius set 0.05 µg/Kg as the regulatory limit)<sup>3</sup>. This has prompted the adoption of regulatory limits in several countries, which, in turn, requires the development of validated official analytical methods for rapid and cost-effective screening of AFM<sub>1</sub> on a large scale.

Currently, several qualitative and quantitative methods have been developed to detect AFM in milk and in dairy products<sup>5-9</sup>. Among them, thin layer chromatography and immune chromatographic assay are the most commonly used methods for rapid qualitative detection and semiquantification of aflatoxins. For examples, the quantification of AFM is usually conducted by high performance liquid chromatography (HPLC) and enzyme linked immunosorbent assay (ELISA)<sup>10,11</sup>. The HPLC fluorimetric detection method can quantify AFM with high accuracy and very low detection limits, but it requires complex and laborious samples pretreatments, such as defatting of milk and subsequent extraction of AFM by methanol or immunoaffinity columns<sup>12,13</sup>. Moreover the chromatographic methods require expensive instrumentatio and skilled operators<sup>13,14</sup>, thus limiting their application, especially in developing countries. In addition, several biosensors have also been developed to analyze

---

the AFM, including electrochemical immunochip sensor and DNA-based electrochemical membrane<sup>15-17</sup>.

The emerging research field of microfluidics provides exciting new possibilities for advanced development of new analytical methods<sup>18-20</sup>. Droplet microfluidic technologies enable to develop a novel biosensor with high control and can tailor the properties of biosensors in a very simple manner to meet the needs of specific applications. However, droplet microfluidics is used only for biomedical and chemical research; limited work has been done for detection of food contaminants using these technologies.

Recently, biorecognition elements (such as enzymes, peptides and antibodies) are used for detection of specific analytes. Several groups have synthesized antibodies for aflatoxin recognition, with high sensitivity<sup>6,21</sup>. The use of these large macromolecules has several limitations, including poor stability and high production costs<sup>22</sup>. In contrast, small molecules like peptides can be prepared synthetically and mimic the antibody binding site by using only a small cluster of residues, even though the affinity and specificity toward biomolecules target result to be lower if compared with antibodies<sup>23</sup>. Based on these considerations, 64 peptides were screened and the sequences which showed the best affinity to aflatoxin were synthesized.

Poly(ethylene glycol) (PEG) is commonly used in biotechnological applications due to its low-fouling and biocompatibility properties. PEG is used to prevent non-specific binding of protein on sensing surface and it is relatively inexpensive<sup>24</sup>. These properties make PEG an attractive material for biosensors intended to work in complex samples without purification, overcoming the complex and laborious steps of samples purification that is typical in the conventional methods. Various approaches have explored PEG's utility as biosensor platform<sup>25</sup>, but we believe that its use in recognition of food contaminants has not yet been developed.

We report a simple, low-cost and label free method for aflatoxin M<sub>1</sub> detection based on microfluidic poly(ethylene glycol) diacrylate (PEGDA) microparticles functionalized with two novel peptides. 64 anti-AFM sequences were screened by Surface Plasmon Resonance (SPR) technique, and the sequences showing best binding affinity ( $K_D = 180 \pm 0.5 \mu\text{M}$  and  $K_D = 172 \pm 0.4 \mu\text{M}$ ) were chosen for our system. AFM<sub>1</sub> capture beads were made from PEGDA microparticles functionalized with the selected peptide moieties. All tests have been performed using AFM<sub>1</sub> conjugated with BSA, because the BSA-conjugation makes the toxin less harmful and easier to manage. AFM<sub>1</sub>-BSA-binding peptides occurred with high affinity

( $K_D$  3.66-6.57 pM, respectively for the two sequences) and detection was demonstrated by fluorescent technique. The results demonstrate that the proposed system system is able to detect levels of AFM<sub>1</sub>-BSA in according with the current legislative requirements of 50 ng/Kg.

The method developed for Streptavidin recognition in complex matrix can be used for aflatoxins detection providing a promising approach for the screening of food contaminates and small molecules.

## ***4.2. Results and discussions***

### ***4.2.1. Peptides sequences characterization***

The first step was the selection of the peptide sequences that has showed the best affinity with AFM<sub>1</sub>. To this end, a preliminary Molecular Docking experiment for studying affinity between AFM<sub>1</sub> and several peptides was performed using Cdocker, an algorithm of Discovery Studios software. Molecular Docking is usually used for the prediction of the preferred orientation of one molecule to a second one when bound to each other to form a stable complex<sup>26</sup>. Knowledge of the preferred orientation in turn may be used to predict the strength of association or binding affinity between the molecules using, that in our case are been peptide and AFM<sub>1</sub>. This part of work is been made in a parallel PhD work, and it is not the object of this one. Briefly, here it is reported a description of the peptides which were chosen for the work.

After Molecular Docking experiment, 64 peptides were synthesized through combinatorial chemistry, for its rapidity and low cost unlike conventional synthetic way of handling one molecule at time<sup>27</sup>. Eight amino acids alanine, arginine, aspartic acid, asparagine, threonine, proline, isoleucine and tryptophan (A,R,D,N,T,P,I,W respectively) were chosen as building blocks, because of their chemical properties (i.e. solubility, different functional groups), their easy availability and their low cost. The amino acids chosen for preparing a library of sufficient size have functional groups in their lateral chains that could not react under our synthesis conditions. To avoid synthetic problems, the composition of the library was simplified by neglecting other amino acids (see experimental section for more details). In this way a known linear amino acid sequence was easily obtained. To estimate the biospecific interaction peptides-aflatoxin a commercially available instrument (SensiQ) was used, which employs the principle of Surface Plasmonic Resonance (SPR). Refractive index changes associated with peptide binding to the aflatoxin-BSA conjugate are detected and quantified

(as response units (RU)) by the instrument as a sensorgram<sup>28</sup>. In our experiments AFM<sub>1</sub>-BSA conjugated as ligand was immobilized on the chip COOH5, achieving 400 RU immobilization level (approximately 1RU is about equal to 1pg/mm<sup>2</sup> of ligand immobilized). Direct binding of each peptide with AFM1 were performed by injecting different concentration of peptides (see Experimental Section). **Figure 4.2** shows the binding of the best two sequences in real-time as a plot of time (seconds) versus response signal (RU) (sensorgrams). The dissociation rates ( $K_D$ ), which define the kinetics and affinities of the interaction, was calculated from these sensorgrams<sup>28</sup>.

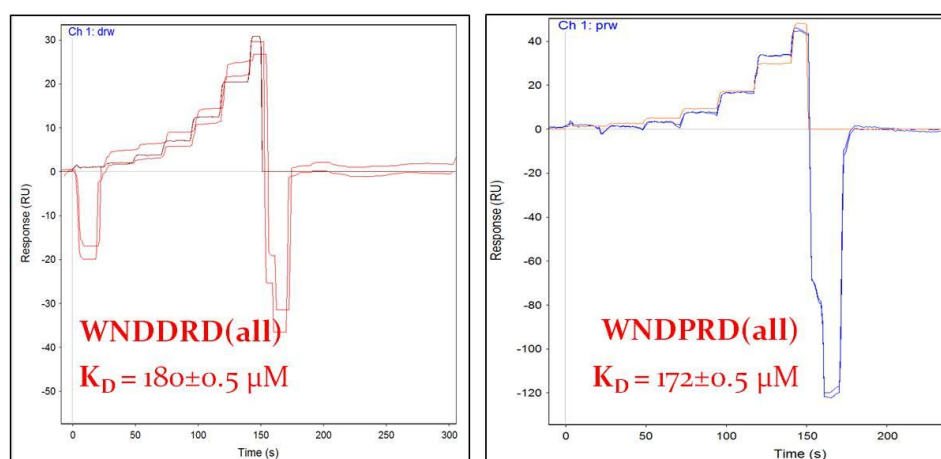


**Figure 4.2:** Sensorgram of response unit versus time illustrating the binding of peptides to immobilized aflatoxinM1-BSA.

SPR offers several advantages over traditional immunoassay techniques for studies of binding interactions. It provides real-time and high throughput monitoring of  $K_D$  with high sensitivity of detection. The two sequences had shown a better sensitivity for AFM<sub>1</sub> than the others, therefore they were chosen as a recognition element for microgels assay development.

#### 4.2.2. Biosensing development

The detection of AFM<sub>1</sub>-BSA was carried out by using microgels after their functionalization with the two novel peptides (WNDDDR(OAll)) and (WNDPRD(OAll)). Both microgels were obtained using similar method, for simplicity, only the procedure for one peptide is showed.

PEGDA peptide-microparticles were synthesized in a flow focusing device. We first demonstrated a distribution of the peptide inside the microgels. For this, the two peptides were fluorescently labeled with rhodamine at the  $\beta$ -alanin (B) site (Rhod-BNDDR(OAll)) and Rhod-BNDPRD(OAll)). The fluorescence images (figure 4.3) show monodisperse

hydrogel particles with a uniform distribution of the labeled peptide within these particles ( $\approx 9.6 \times 10^{-3}$  pg of peptide per microparticle), results that are similar to our previous work (chapter 3).

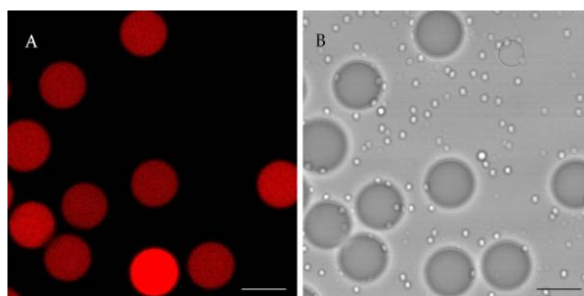


**Figure 4.3:** PEGDA-peptide microgel with (Rhod-BNDDRD(OAll)). A) Fluorescent image of (Rhod-BNDDRD(OAll) encapsulated; B) Phase contrast image of microgels. Scale bars are 30  $\mu\text{m}$ .

Peptide (without rhodamine) was mixed with PEGDA solution before synthesis and PEGDA peptide-microparticles were formed by a continuous microfluidic procedure (described in Chapter 3). Briefly, the pre-polymer solution containing peptide, a disperse phase, was injected through the central channel of the microfluidic device and oil solution with surfactant, a continuous phase, was injected through two side channels. Under optimized flow rate conditions disperse phase was sheared into monodisperse droplets by continuous phase. The obtained PEGDA peptide-microgels are monodisperse in size with a coefficient of polydispersity (PDI)  $< 0.003$ .

PEGDA has been chosen for its resistance to protein adsorption. Peptide retains its structure (random-coil as it expect for small peptides) after its encapsulation, as previously reported for other peptides<sup>29</sup> and confirmed in our previous work (chapter 3).

Detection through fluorescence relies on the presence of a chromophore in the molecules, and AFs already have natural fluorescence (**Figure 4.4**) and can be detected directly with fluorescence techniques<sup>30</sup>.

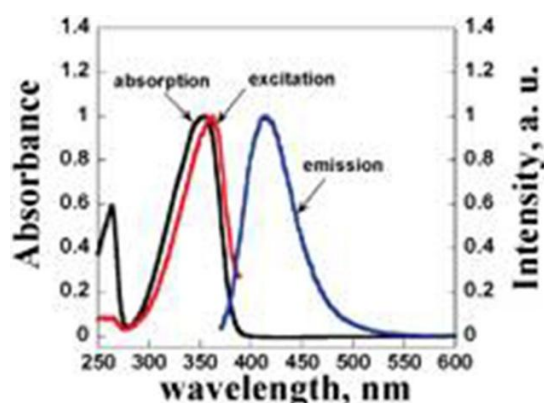


**Figure 4.4:** Normalized ground state absorption, excitation and emission spectra for aflatoxin.

As shown in **Figure 4.5** the fluorescence intensity increased with the increase of AFM<sub>1</sub>-BSA concentration in both experiments. **Figure 4.5** also shows a correlation between fluorescent signal and AFM<sub>1</sub>-BSA level (ng/Kg) in the dynamic range from 3.28 ng/Kg to 70 ng/Kg. We also observed that there was no obvious change of fluorescent intensity when the concentration of AFM<sub>1</sub>-BSA is higher than 70 ng/Kg. Thus the saturation point of AFM<sub>1</sub>-BSA is at 70 ng/Kg in PBS. The results demonstrate the highly sensitivity of this method with an estimated  $K_D$  of  $3.66 \pm 1.55$  and  $6.57 \pm 3.95$  pM respectively for (WNDDR(OAll)) and (WNDPR(OAll)), which obviously make a good affinity toward AFM<sub>1</sub>-BSA. Moreover, our system is able to detect levels of AFM<sub>1</sub>-BSA in according with the current legislative requirements of 50ng/L.

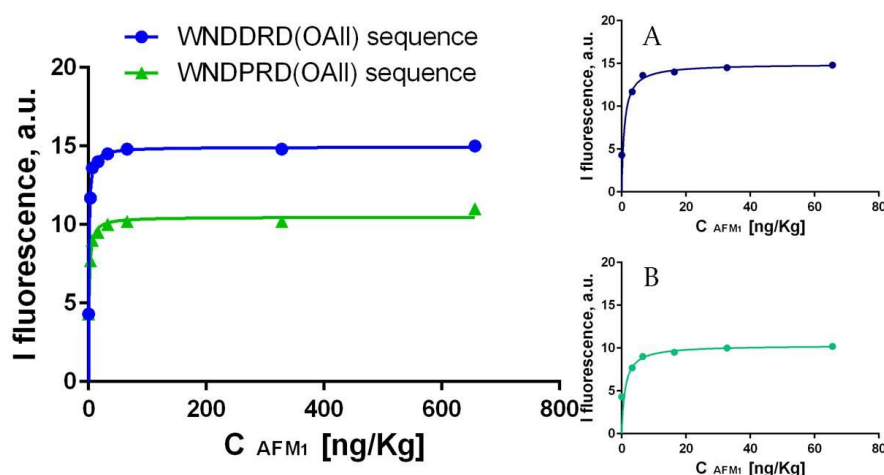


**Figure 4.5:** Correlation between fluorescent signal and AFM<sub>1</sub>-BSA level (ng/Kg) in the sample. A) zoom for (WNDDR(OAll))-AFM<sub>1</sub>-BSA binding in the range from 3.28 and 65 ng/Kg. B) zoom for (WNDPR(OAll))-AFM<sub>1</sub>-BSA binding in the range from 3.28 and 65 ng/Kg.

Further, we synthesized microgels without peptide (a negative control) and performed the same protocol. As shown in **Figure 4.6**, PEGDA microgels without peptide did not show a significant fluorescent signal compared to functionalized microgels, demonstrating the high specificity of peptide-microgels assay.

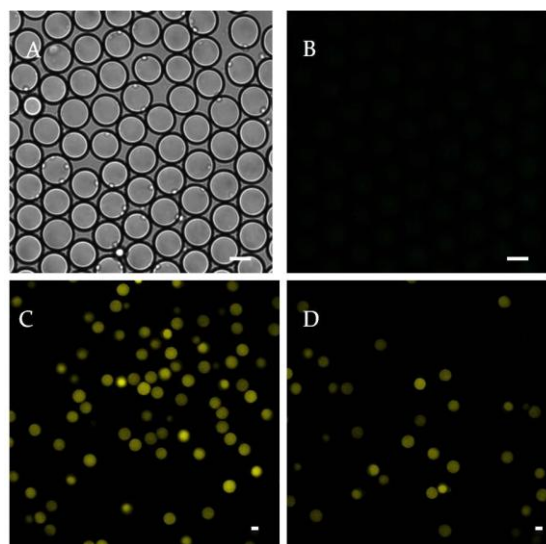


**Figure 4.6:** AFM<sub>1</sub> detection confocal results. A) bright field and B) fluorescent images of AFM<sub>1</sub>-binding microparticles without peptide; C) fluorescent images of WNDPRD(OAll)-microgels binding and D) WNDPRD(OAll)-microgels binding. Different zoom is used, scale bar 30  $\mu\text{m}$ .

The demonstrated method is an attractive alternative for AFM<sub>1</sub> detection and quantification due to its specificity and reproducible properties of hydrogel particles. Importantly, our strategy is relatively simple and robust, and encapsulated molecules retain their structure during microgels processing. For the first time small molecules were used for AFMs detection and the functionalization of the microgels is provided directly in flow, avoiding the long and time-consuming steps that characterize conventional techniques<sup>31</sup> for microgels functionalization.

The work reported here is an initial investigation into developing new technology in food contaminants detection; the work is still in progress and gives “proof-of-concept” of the technology for an important application.

### ***4.3. Conclusion***

In this work, we report a novel method for label-free and sensitive monitoring of AFM<sub>1</sub> by using microfluidic functional microgels in PBS. Compared with conventional techniques, such as HPLC or ELISA, the peptide-microgels strategy is simple, sensitive, and specific,

without the need for multiple sample preparation or separation steps or a skilled operator. We believe that the reported system could be applicable for rapid AFM<sub>1</sub> detection in milk, due to PEGDA property to prevent non-specific binding of proteins on sensing surface.

#### ***4.4. Acknowledgments***

The experiment performed in this chapter were performed in collaboration with Concetta Di Natale, who developed peptide synthesis protocol and performed SPR experiment. Vincenzo Calcagno is gratefully acknowledged for fruitful discussion.

#### ***4.5. Experimental Section***

*General Materials and Method.* Poly(ethylene glycol) diacrylate (PEGDA, 700 MW), the non polar solvent light mineral oil and the nonionic detergent sorbitan monooleate (Span 80) were purchased from Sigma Aldrich. Crosslinking reagent Darocur 1173 was purchased from Ciba. Reagents for peptide synthesis (Fmoc-protected amino acids, resins, activation, and deprotection reagents) were purchased from Iris Biotech GmbH (Waldershofer Str. 49-51 95615 Marktredwitz, Deutschland) and InBios (Naples, Italy). Solvents for peptide synthesis, HPLC analyses and AFM<sub>1</sub>-BSA conjugate (4-8 mol AFM per mol BSA) were purchased from Sigma-Aldrich; reversed phase columns for peptide analysis and the LC-MS system were supplied respectively from Agilent Technologies and Waters (Milan, Italy). Pooled human serum from healthy donors was supplied by Lonza (Life Technology Ltd, Paisley, UK). All chemicals were used as received.

*Microfluidic device fabrication.* Microfluidic device consists of two inlets for the continuous and disperse phase, a narrow orifice in which the main channel and the two opposite channels converge, and a serpentine in which droplets were polymerized. The dimensions of the microchannel dimensions in the region of droplet formation is  $50 \times 35 \times 50$  (width  $\times$  depth  $\times$  length); the serpentine is 10 cm long. The microfluidic device was fabricated by combining the conventional photolithographic and soft-lithographic techniques. Briefly, negative photoresist (Mr-DWL 40 photoresist, Microresist technology) was spun onto a silicon wafer at 2000 rpm for 30 s to make a 35  $\mu$ m thick layer of photoresist. The photoresist was baked and subsequently exposed using DWL 66 Fs LASER technology system (Heidelberg instruments). After the exposed sample had been post-baked and developed, the microfluidic flow focusing device master was prepared. The surface of the device mold was treated with tridecafluoro-1,1,2,2-tetrahydrooctyl-1-trichlorosilane to facilitate the removal of a

---

polydimethyl-siloxane (PDMS, Sylgard 184, Dow Corning) replica. PDMS (10:1 polymer to curing agent) was poured on the patterned silicon wafer containing negative-channels. The PDMS-based microfluidic device was peeled off from the wafer, treated with oxygen plasma and bonded with a glass slide.

*Synthesis of peptides.* Peptide libraries and single peptides were prepared by the solid phase method on a 50  $\mu\text{mol}$  scale following the Fmoc strategy and using standard Fmoc-derivatized amino acids. Briefly, synthesis were performed on a fully automated multichannel peptide synthesizer Biotage® Syro Wave™. RINK AMIDE resin (substitution 0.71 mmol/g) was used as solid support. Activation of amino acids was achieved using HBTU-HOBt-DIEA (1:1:2), whereas Fmoc deprotection was carried out using a 40% (v/v) piperidine solution in DMF. All coupling reactions were performed for 15 minutes and deprotection reactions for 10 minutes. 8 different amino acids (Arg, Asn, Pro, Trp, Leu, Ala, Asp and Thr) were chosen to build a peptide library based on their chemical and physical properties. The solid phase (4,55g) was split into 64 different tubes and each reactor holds the combination of the eight amino acids, selected for the library construction, as first and second coupling. At the end of coupling procedure previously reported; we obtained 64 different di-peptides that constituted the first peptide library. The di-peptide with the best binding properties (selected by SPR technique) was chosen as an initial solid phase for the second library. We prepared 4,55 g of the resin with the selected dipeptide immobilized on its surface by the same solid phase synthesis described procedures. We split this new solid phase into 64 different tubes and we bound a third amino acid to the activated  $\alpha$ -carboxylic group of the second amino acid. The synthesis steps were the same as those followed for the first and second amino acid. At the end a fourth amino acid was linked to the third one by the same synthesis procedures. We obtained 64 tetrapeptides that had the same first and second amino acid but different third and fourth one and that constituted our second and last library. The best binding tetra-peptides, selected by SPR, were rhodamine to monitor their entrapment in microparticles. Lysine side chain amine rhodamine labeling was achieved by on-resin treatment with rhodamine isothiocyanate (TRITC) after removing methyltrityl (Mtt) protecting group using 1% TFA in DCM for 30 min.

*SPR analysis.* The interactions between all 64 di-peptide and tetra-peptide were measured using SPR technique with SensiQ Pioneer from AlfaTest (Rome, Italy). In order to measure the affinity of the peptides (analyte) with the aflatoxin (ligand), AFM<sub>1</sub>-BSA conjugated was immobilized at a concentration of 50  $\mu\text{g}/\text{mL}$  in a 10 mM acetate buffer pH 3.7 (flow 10

$\mu\text{L}/\text{min}$ , injection time 20 min) on a COOH1 SensiQ sensor chip, using EDC/NHS chemistry (0.4 M EDC - 0.1 M NHS, flow  $25\mu\text{L}/\text{min}$ , injection time 4 min), achieving a 7000 RU signal. The reactive residues were deactivated by treatment with ethanolamine hydrochloride 1 M, pH 8.5. In order to study the aspecific binding of peptides against BSA, the reference channel was prepared by activation with EDC/NHS and immobilized the only BSA at a concentration of  $50\mu\text{g}/\text{mL}$  and reaching the same RU signal of the toxin (7000). The binding assays were performed at  $25\mu\text{L}/\text{min}$ , with a contact time of 4 min, all peptides were diluted in the stock buffer, HBS (10 mM Hepes, 150 mM NaCl, 3 mM EDTA, pH 7.4). The injection of analytes (100  $\mu\text{l}$ ) was performed at the indicated concentrations. The association phase ( $k_{\text{on}}$ ) was followed for 180 s, whereas the dissociation phase ( $k_{\text{off}}$ ) was followed for 300 s. The complete dissociation of the formed active complex was achieved by addition of 10 mM NaOH, for 60 s before starting each new cycle. To subtract the signal of the reference channel and evaluate the kinetic and thermodynamic parameters of the complex, the software QDAT analysis package (SensiQ Pioneer, AlfaTest) was used. For tetra-peptide library binding experiment was conducted by Fast step injection. Fast Step is an in situ-dilution method that enables stepped analyte gradient injections to be performed where the concentration of sample steps up, or down, according to a predefined profile without reliance on dispersive mixing in a flow channel. The analyte concentration is modulated en route to the flow cell on-the-fly. This eliminates the overhead associated with multiple loading, injecting and clean up cycles making possible substantial reductions in experimental time and complexity. The dissociation of analyte can be accurately estimated from a single dissociation phase curve recorded after the step injection is complete. The sample throughput can be increased by >10-fold compared to conventional methods. In this case an analyte concentration of 1mM was used with a flow rate of  $200\mu\text{L}/\text{min}$ , a contact time of 20 sec and a dissociate time of 120 sec. As for bulk standard cycles, a 20% of sucrose was used. In all experiments kinetic parameters for all tetra-peptides were estimated assuming a 1:1 binding model and using QDAT software (SensiQ Technologies).

*Synthesis of functional microgels.* Microgels were synthesized using light mineral oil containing nonionic surfactant Span 80 (3 wt%) as a continuous phase and poly(ethylene glycol)diacrylate (PEGDA) (20 wt%) with photoinitiator (0.1 wt%) and peptides (70 mg/L) as a disperse phase. Droplets were formed injecting prepolymer solution, disperse phase, through the central channel and oil solution, continuous phase, through two opposite side channels. The uniform PEGDA-peptide droplets were crosslinked in flow to form monodisperse

microgels. On average droplets were exposed to UV light for 15s. The UV light (9.8 mW) was filtered with DAPI microscopy filter ( $\lambda=360$  nm) and focused on the device. The diaphragm aperture of the microscope was used to limit exposure to the serpentine region of the chip. After photopolymerization, microgels were collected in an eppendorf and washed three times with a solution of ethanol (35 v/v%) and acetone (10 v/v%) to remove the oil. The device inlets and outlets were connected with polyethylene tubes, and the solutions were injected using high-precision syringe pumps (neMesys-low pressure) to ensure a reproducible, stable flow. This system was mounted on an inverted microscope (IX 71 Olympus) and droplet formation was visualized using a 4 $\times$  objective and recorded with a CCD camera Imperx IGV-B0620M.

*Protocol of peptides encapsulation and AFM<sub>1</sub>-BSA detection.* Microgel was functionalized by adding the selected peptide (WNDDRD(OAll) or WNDPRD(OAll)) in the disperse phase prior to a microgel synthesis. Binding experiments were performed incubating peptides-microgels with AFM<sub>1</sub>-BSA in PBS (pH 7.4) (final volume 100  $\mu$ L) at room temperature for 2 h. 5  $\mu$ L of peptide-microgels were suspended in 100  $\mu$ L of PBS and different concentrations of AFM<sub>1</sub>-BSA, ranging from 3.28 ng/Kg to 656 ng/Kg, were added. After the incubation, microgels were washed and their fluorescence were analyzed by confocal. The same protocol was used for microgels without peptide, as a negative control.

*Confocal Microscopy.* Fluorescence analysis of protein-binding were performed by Leica SP5 confocal microscope (Leica Microsystems), provided with an HCX IRAPO L 25.0 $\times$ /0.95 WATER objective and a 360 nm as selected wavelength as excitation sources for AFM<sub>1</sub>-BSA. Detection occurred at the 420-450 nm band. Images have been acquired with a resolution of 1024  $\times$  1024 pixels, zoom 1, 2.33 A.U. pinhole. All our experiments were performed at room temperature.

*Statistical analysis.* The results of confocal experiments were analyzed by software GraphPad Prism version 5.04 and experimental data were expressed as mean  $\pm$  standard deviation. The evaluation of  $K_D$  was calculated by a non-linear fitting approach using GraphPad Prism version 5.04 software.

*Safety.* Aflatoxins are powerful hepatotoxins and carcinogens, so great care should be taken to avoid personal exposure and potential laboratory contamination. All items coming in contact with aflatoxins (glassware, vials, tubes, etc.) were immersed in a 10% bleach solution for 1-2h before they were discarded. Pure aflatoxin standard was handled in a hood with extreme caution.

---

### References

- 1 Asi, M. R., Iqbal, S. Z., Ariño, A. & Hussain, A. Effect of seasonal variations and lactation times on aflatoxin M 1 contamination in milk of different species from Punjab, Pakistan. *Food Control* **25**, 34-38 (2012).
- 2 Fallah, A. A., Jafari, T., Fallah, A. & Rahnama, M. Determination of aflatoxin M1 levels in Iranian white and cream cheese. *Food and chemical toxicology* **47**, 1872-1875 (2009).
- 3 Iqbal, S. Z., Jinap, S., Pirouz, A. & Faizal, A. A. Aflatoxin M 1 in milk and dairy products, occurrence and recent challenges: A review. *Trends in Food Science & Technology* **46**, 110-119 (2015).
- 4 Iqbal, S. Z. *et al.* Aflatoxin B1 in chilies from the Punjab region, Pakistan. *Mycotoxin research* **26**, 205-209 (2010).
- 5 Tang, D., Liu, B., Niessner, R., Li, P. & Knopp, D. Target-induced displacement reaction accompanying cargo release from magnetic mesoporous silica nanocontainers for fluorescence immunoassay. *Analytical chemistry* **85**, 10589-10596 (2013).
- 6 Wang, Y. *et al.* Isolation of alpaca anti-idiotypic heavy-chain single-domain antibody for the aflatoxin immunoassay. *Analytical chemistry* **85**, 8298-8303 (2013).
- 7 Li, X. *et al.* Molecular characterization of monoclonal antibodies against aflatoxins: a possible explanation for the highest sensitivity. *Analytical chemistry* **84**, 5229-5235 (2012).
- 8 Parker, C. O., Lanyon, Y. H., Manning, M., Arrigan, D. W. & Tothill, I. E. Electrochemical immunochip sensor for aflatoxin M1 detection. *Analytical chemistry* **81**, 5291-5298 (2009).
- 9 He, T. *et al.* Nanobody-based enzyme immunoassay for aflatoxin in agro-products with high tolerance to cosolvent methanol. *Analytical chemistry* **86**, 8873-8880 (2014).
- 10 Bognanno, M. *et al.* Survey of the occurrence of aflatoxin M1 in ovine milk by HPLC and its confirmation by MS. *Molecular nutrition & food research* **50**, 300-305 (2006).
- 11 Santini, A., Ferracane, R., Meca, G. & Ritieni, A. Comparison and improvement of the existing methods for the determination of aflatoxins in human serum by LC-MS/MS. *Analytical Methods* **2**, 884-889 (2010).
- 12 Hussain, I., Anwar, J., Asi, M. R., Munawar, M. A. & Kashif, M. Aflatoxin M 1 contamination in milk from five dairy species in Pakistan. *Food Control* **21**, 122-124 (2010).
- 13 Kraiczek, K. G., Rozing, G. P. & Zengerle, R. Relation between chromatographic resolution and signal-to-noise ratio in spectrophotometric HPLC detection. *Analytical chemistry* **85**, 4829-4835 (2013).
- 14 Soloshonok, V. A., Roussel, C., Kitagawa, O. & Sorochnikov, A. E. Self-disproportionation of enantiomers via achiral chromatography: a warning and an extra dimension in optical purifications. *Chemical Society Reviews* **41**, 4180-4188 (2012).
- 15 Banitaba, M. H., Davarani, S. S. H. & Mehdinia, A. Study of interactions between DNA and aflatoxin B1 using electrochemical and fluorescence methods. *Analytical biochemistry* **411**, 218-222 (2011).
- 16 Siontorou, C. G., Nikolelis, D. P., Miernik, A. & Krull, U. J. Rapid methods for detection of Aflatoxin M 1 based on electrochemical transduction by self-assembled metal-supported bilayer lipid membranes (s-BLMs) and on interferences with transduction of DNA hybridization. *Electrochimica acta* **43**, 3611-3617 (1998).

- 17 Tombelli, S., Mascini, M., Scherm, B., Battacone, G. & Migheli, Q. DNA biosensors for the detection of aflatoxin producing *Aspergillus flavus* and *A. parasiticus*. *Monatshefte für Chemie-Chemical Monthly* **140**, 901-907 (2009).
- 18 Fairhead, M. *et al.* SpyAvidin hubs enable precise and ultrastable orthogonal nanoassembly. *Journal of the American Chemical Society* **136**, 12355-12363 (2014).
- 19 Leontis, N. B. & Westhof, E. Self-assembled RNA nanostructures. *Science* **345**, 732-733 (2014).
- 20 Jagadeesh, R. V., Junge, H. & Beller, M. Green synthesis of nitriles using non-noble metal oxides-based nanocatalysts. *Nature communications* **5** (2014).
- 21 Hou, P. *et al.* Pluripotent stem cells induced from mouse somatic cells by small-molecule compounds. *Science* **341**, 651-654 (2013).
- 22 Chirinos-Rojas, C. L., Steward, M. W. & Partidos, C. D. A peptidomimetic antagonist of TNF- $\alpha$ -mediated cytotoxicity identified from a phage-displayed random peptide library. *The Journal of Immunology* **161**, 5621-5626 (1998).
- 23 Banner, D. W. *et al.* Crystal structure of the soluble human 55 kd TNF receptor-human TNF $\beta$  complex: implications for TNF receptor activation. *Cell* **73**, 431-445 (1993).
- 24 Urban, G. & Weiss, T. in *Hydrogel Sensors and Actuators* 197-220 (Springer, 2010).
- 25 Mehne, J. *et al.* Characterisation of morphology of self-assembled PEG monolayers: a comparison of mixed and pure coatings optimised for biosensor applications. *Analytical and bioanalytical chemistry* **391**, 1783-1791 (2008).
- 26 Lengauer, T. & Rarey, M. Computational methods for biomolecular docking. *Current opinion in structural biology* **6**, 402-406 (1996).
- 27 Tozzi, C., Anfossi, L., Baggiani, C., Giovannoli, C. & Giraudi, G. A combinatorial approach to obtain affinity media with binding properties towards the aflatoxins. *Analytical and bioanalytical chemistry* **375**, 994-999 (2003).
- 28 Daly, S. J. *et al.* Development of surface plasmon resonance-based immunoassay for aflatoxin B1. *Journal of Agricultural and Food Chemistry* **48**, 5097-5104 (2000).
- 29 Black, K. A. *et al.* Protein encapsulation via polypeptide complex coacervation. *ACS Macro Letters* **3**, 1088-1091 (2014).
- 30 Valenta, H. Chromatographic methods for the determination of ochratoxin A in animal and human tissues and fluids. *Journal of Chromatography A* **815**, 75-92 (1998).
- 31 Causa, F., Aliberti, A., Cusano, A. M., Battista, E. & Netti, P. A. Supramolecular spectrally encoded microgels with double strand probes for absolute and direct miRNA fluorescence detection at high sensitivity. *Journal of the American Chemical Society* **137**, 1758-1761 (2015).

### *5.1. Conclusions and outlook*

Microdroplets in microfluidics has become a fast moving research area that is rapidly being established as a powerful tool for complex chemical and biological experiments<sup>1</sup>. Crucial to this progress has been the development of simple modules for the manipulation of droplets in the past 10 years. Monodisperse droplets can now be generated and manipulated on-fluidic chip (including heating, cooling, fusing, mixing, storing, sorting, etc.) essential for carrying out experiments in bulk<sup>2</sup>.

Compartmentalization is clearly a powerful concept for isolating and studying single cells and their environments<sup>3,4</sup>. Microfluidic droplets are monodisperse, can be formed and analyzed at sufficiently large numbers, and manipulated efficiently while containing the small amounts of cellular material uncontaminated within those droplets. Integrated devices coupled to highly sensitive, ideally label-free detection methods, provide a new tool for exploring single-cell genomics, proteomics, and for food contaminants detection, which are research areas our findings contribute to.

Droplet-based microfluidics has allowed for the study of rare tumor cells and circulating tumor cells (CTCs) in progressively more cell-like systems. CTCs are typically detected by immunomagnetic separation methods [Cellsearch], which require laborious operating steps and may result in the loss of target cells<sup>5</sup>. Our approach, contributes the field of cancer research providing a robust and label-free method to CTCs detection, without damaging them, thus opens new routes to further characterization of CTCs as key for therapeutic targets identification. We show that cancer cell metabolism, and more specifically, both the acidification of the extracellular microenvironment and the Warburg effect<sup>6</sup>, can be used to identify and count rare tumor cells and CTCs. Further work is needed to clarify how these results could impact in clinical routine. CTCs nature could be characterized for predicting cancer progression, achieving personalized cancer treatments and monitoring their efficacy.

On the other side droplet microfluidics allows for the production of functional microparticles as biosensors<sup>7,8</sup>. The use of microfluidics has allowed the synthesis of new class of microparticles with novel shape, compartments and microstructures, which are very difficult to achieve using the conventional bulk emulsification methods. Our work provides innovative

---

advances in gel particle functionalization and opens new possibilities for direct molecules detection in complex fluids. We show how the compartmentalization of small analytes and the choose of polyethylene glycol (PEG), for its antifouling property, improve the sensitivity and the specificity of the detection system. We developed a label-free strategy to detect aflatoxin. It is typically screened by chromatographic methods, which need multiple separation steps of the sample and require skilled operators<sup>9</sup>. Microparticles strategy is simple and sensitive and could be applicable for direct aflatoxin detection in milk thanks to PEG property to prevent non-specific binding of protein on sensing surface. More works in this area could be directed towards its clinical integration forward from current “proof-of-concept”. The next step therefore is to use this method to aflatoxin detection directly in milk.

The systems we described may provide some improving in the actual research on cancer and food contaminants screening. The using of microfluidics has followed for the develop of robust, label-free, sensitive and high-throughput platforms which we hope will be used in the near future to improve the quality of life.

### ***Publications:***

G.Celetti, C.Di Natale, F.Causa, E. Battista, P.A. Netti. Functionalized poly(ethylene glycol) microgels by microfluidics: in situ peptide encapsulation for in serum selective protein detection. *Colloids and Surfaces B: Biointerfaces*. DOI: 10.1016/j.colsurfb.2016.04.036

Fabio Del Ben, Matteo Turetta<sup>†</sup>, Giorgia Celetti, Aigars Piruska, Michela Bulfoni, Daniela Cesselli, Wilhelm T.S. Huck\*, Giacinto Scoles. A method for detecting circulating tumor cells based on measurement of single cell metabolism in droplet-based microfluidics. *Angewandte Chemie*. DOI: 10.1002/anie.201602328R1

---

### References

- 1 Theberge, A. B. *et al.* Microdroplets in microfluidics: an evolving platform for discoveries in chemistry and biology. *Angewandte Chemie International Edition* **49**, 5846-5868 (2010).
- 2 Guo, M. T., Rotem, A., Heyman, J. A. & Weitz, D. A. Droplet microfluidics for high-throughput biological assays. *Lab on a Chip* **12**, 2146-2155 (2012).
- 3 Huebner, A. *et al.* Development of quantitative cell-based enzyme assays in microdroplets. *Analytical chemistry* **80**, 3890-3896 (2008).
- 4 Brouzes, E. *et al.* Droplet microfluidic technology for single-cell high-throughput screening. *Proceedings of the National Academy of Sciences* **106**, 14195-14200 (2009).
- 5 Steen, S., Nemunaitis, J., Fisher, T. & Kuhn, J. Circulating tumor cells in melanoma: a review of the literature and description of a novel technique. *Proceedings (Baylor University Medical Center)* **21**, 127 (2008).
- 6 Vander Heiden, M. G., Cantley, L. C. & Thompson, C. B. Understanding the Warburg effect: the metabolic requirements of cell proliferation. *science* **324**, 1029-1033 (2009).
- 7 Seiffert, S., Thiele, J., Abate, A. R. & Weitz, D. A. Smart microgel capsules from macromolecular precursors. *Journal of the American Chemical Society* **132**, 6606-6609 (2010).
- 8 Seiffert, S., Romanowsky, M. B. & Weitz, D. A. Janus microgels produced from functional precursor polymers. *Langmuir* **26**, 14842-14847 (2010).
- 9 Ellis, W., Smith, J., Simpson, B., Oldham, J. & Scott, P. M. Aflatoxins in food: occurrence, biosynthesis, effects on organisms, detection, and methods of control. *Critical Reviews in Food Science & Nutrition* **30**, 403-439 (1991).

---

## *Acknowledgments*

Poche ore alla sottomissione della tesi per i referee, e la paura che possa andare diversamente da quanto ci si aspetti c'è, sono sincera. I ringraziamenti sono la parte più attesa dal pubblico ... quindi, cominciamo.

I feel to thank all people who supported and helped me during these 3 years.

I would like to thank professor Wilhelm Huck for teaching me that if working with constancy and commitment great satisfaction would come. Thank you because you have filled my days of knowledge, thank you for this great opportunity.

Another thanks goes to Aigars. Thank you! Thank you for teaching me what means working in a group, that the comparison is necessary for growth. Thanks for your patience, for the coffee breaks, for helping me when I was discouraged. Thanks for the help that you have given me in the last month so “special”, it was a real pleasure working with you!

La mia famiglia. Grazie per avermi aiutata a crescere, a credere che tutto è possibile se ci si crede veramente. Grazie per avermi insegnato che i sacrifici sono necessari ma ripagano. Grazie per avermi dato la libertà di scegliere chi diventare. Grazie, perché non mi avete mai fatta sentire sola, anche a 1800 km di distanza, e grazie per aver fatto l'impresa titanica di venire in Olanda con la macchina, sfidando la neve e il freddo! Grazie sister. Ci sei sempre stata. Da quando siamo cresciute sento questa incredibile sensazione che potrò sempre contare su una persona. E quella persona sei tu. Alcuni amori passano, altri più fortunati restano e ci accompagnano per il resto della vita, ma tu sei quella persona che c'è sempre stata e sempre ci sarà. Quindi grazie.

I would to thank my friends. A chi c'è sempre stato Rosita, Giada, Alessandra, Martina, Nicola, Mario, Giovanni and Savo, all in a different way you have helped me and given nice days. Thanks to the friends that I met in these last three years: Pulcino (a te va un grazie particolare), Titti, Elisa, Chiara, Gianluigi, Armando, Domenico, Britta, Stephanie, Florian (thanks for WBC :P): Ilia, Maaruthy, Sjoerd, Joest, Albert. Thanks for the moments that we spent out of the lab and for the fruitful scientific discussions that have helped me to grow. Thanks for the good memories that I will keep in my heart forever.

E poi...grazie a te. Grazie perché hai creduto sempre in me. Grazie per avermi insegnato che la forza sta nella gentilezza, e la grandezza nell'altruismo. Grazie per tutte le volte che mi hai aiutata a superare momenti difficile e grazie per aver scaldato il mio cuore quando rischiava di

---

diventare freddo come la neve. Grazie per i bei momenti, le passeggiate sul mare, le risate, le gite, i concerti, i consigli scientifici. Grazie per tutto il tempo che mi hai dedicato e che hai reso speciale. Grazie Soda.

Un grazie va anche alla dottoressa Marinella, perché è stata l'unica dall'Italia che mi ha aiutata (anche se il suo ruolo prevedeva "solo" l'aspetto burocratico del dottorato) a portare avanti questo PhD.